Atmospheric Pollution Research xxx (xxxx) xxx–xxx

HOSTED BY

Contents lists available at ScienceDirect

Atmospheric Pollution Research

journal homepage: www.elsevier.com/locate/apr

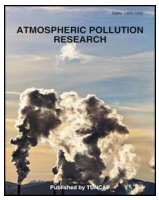

Influence of fireworks emission on aerosol aging process at lower troposphere and associated health risks in an urban region of eastern central India

Mithlesh Mahilang[a], Manas Kanti Deb[a,*], Jayant Nirmalkar[a,b], Shamsh Pervez[a]

[a] School of Studies in Chemistry, Pt. Ravishankar Shukla University, Raipur, 492010, Chhattisgarh, India
[b] Korea Research Institute of Standards and Science, Daejeon, 34113, South Korea

ARTICLE INFO

Keywords:
Deepawali festival
Size-distribution
Aerosol aging
Inhalation dose
Potential penetration
Health impacts

ABSTRACT

To study the influence of fireworks in atmospheric aerosols and their effect on health during the extreme firework days, fireworks tracer metals and carbonaceous species in size-distributed aerosols in the lower troposphere at Raipur in eastern central India were investigated during the 2018 Deepawali festival. Aerosol samples were collected, before Deepawali period (BDP, n = 5), during Deepawali period (DDP, n = 5) and after Deepawali period (ADP, n = 5). Bimodal size-distribution with intense fine mode peak was found for Na during DDP. Bimodal distribution with fine mode intense peak was found for K during DDP. The bimodal size distribution of K was found common for other events because of biomass burning emissions, whereas high intense peak during DDP indicated mixed sources from biomass burning and fireworks. During DDP, K and Ca were well correlated (r^2 = 0.93) together. Strong metal-metal correlations were found between the following pairs, Zn–Fe, Cu–Fe and Cu–Ca, which indicated the similar firecrackers burning source. The atmospheric aging of aerosols was also found significantly high during fireworks days. Aging of aerosols were higher because of heterogeneous reactions of SO_2 and NO_x on aerosols directly emitted from fireworks. The observed high values of inhalation dose of elemental carbon during DDP period imposed higher risk of respiratory diseases. This study has provided carbonaceous fractions composition data as a tool to detect the aging processes of fireworks in ultra-fine, fine and coarse mode particles during the extreme firework days. Inhalation doses were calculated to establish potential influence on human health.

1. Introduction

Atmospheric aerosols released from firecrackers burning in special occasion or festival time around the world have acquired greater attention such as Guy Fawkes night in the United Kingdom (Allan et al., 2010), Deepawali festival in India, Lantern festival in China, New Year's celebration in United States, Firecrackers festival of Taiwan, Maltese archipelagos festas celebration and Las Fallas celebration of Spain (Moreno et al., 2007; Wang et al., 2007; Camilleri and Vella, 2010; Do et al., 2012; Nirmalkar et al., 2016; Li et al., 2017). In spite of eye-catching colorful visual appearance in the sky with the continuous sound of detonation of firecrackers, this short-term emission, results in large airborne gaseous as well as particle pollutants in the troposphere (Pongpiachan et al., 2017; Bencardino et al., 2018). This emission leads to serious environmental implications, which results in the deterioration of health quality and life expectancy. For instance, due to severe airborne pollution in China, the government has declared a ban on manufacturing, sales and bursting of firecrackers in some cities from 1993 to 2006 to overcome such situations (Han et al., 2007). In New Delhi worst atmospheric condition was observed during November 2017, because of sudden rise in particulate matters due to local as well as transported pollutants, which reduced the visibility to less than 50 m, and people faced health problems like coughing, eyes watering, difficulties in breathing and headaches. Apropos to the above government declared a health emergency in Delhi during November 2017 (Terry et al., 2018). Conticini et al. (2020) conducted a correlation-based study between the fatality rate of Severe Acute Respiratory Syndrome CoronaVirus 2 (SARS-CoV2) and the level of atmospheric pollution. They reported study site with high atmospheric pollution were having high fatality rate in the people suffering from SARS-CoV2 viral infection.

Carbonaceous aerosols have drawn greater attentions of researchers

Peer review under responsibility of Turkish National Committee for Air Pollution Research and Control.
* Corresponding author.
E-mail address: debmanas@yahoo.com (M.K. Deb).

https://doi.org/10.1016/j.apr.2020.04.009
Received 8 February 2020; Received in revised form 17 April 2020; Accepted 17 April 2020

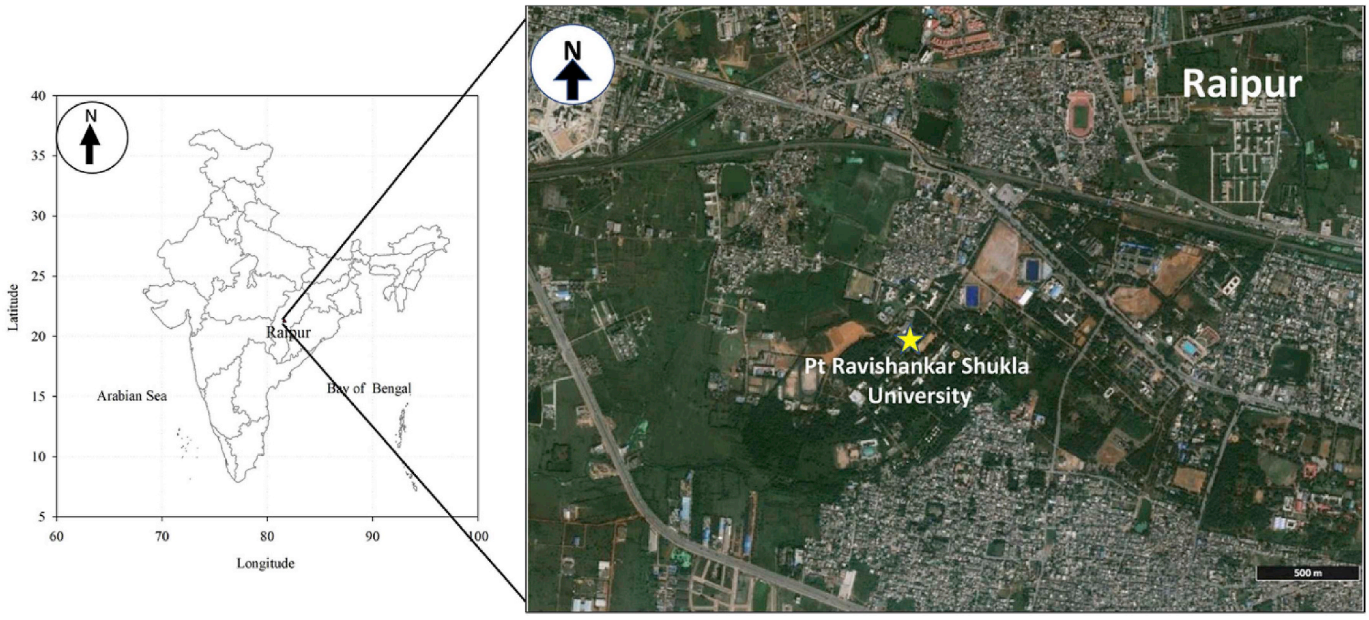

Fig. 1. Study site-Raipur Chhattisgarh, India, is situated between 22° 33′ to 21° 14′ N latitude and 82° 6′ to 81° 38′ E longitude.

because carbonaceous aerosols cover major fraction of atmospheric aerosols and their negative environmental implication as well as severe human health problems are associated with it (Bisht et al., 2015; Liu et al., 2016). Many researchers have reported that carbonaceous fractions of aerosols contribute more than other fractions of aerosols like inorganic and ionic components in troposphere (Tao et al., 2013; Li et al., 2014). Carbonaceous aerosols are of two types, i.e., elemental carbon (EC) and organic carbon (OC). The EC are mainly emitted from the incomplete combustion of carbon containing substances, e.g., fossil fuel and biomass (Wang et al., 2018). Whereas, OCs are either emitted directly from re-suspension of soil containing degraded biomass, biomass burning, vehicular and coal-based industrial exhausts, etc., as primary sources or they can be formed as secondary pollutants or secondary organic aerosols from varieties of chemical reactions through photochemical oxidation of gaseous precursors such as volatile organic compounds (Turpin and Huntzicker, 1991; Koelmans et al., 2006; Bisht et al., 2015). It can be stated that OC may be consisted of primary organic carbon (POC) or it may be the product of heterogeneous chemical reactions as secondary organic carbon (SOC) during gas to particle conversion process.

India is one of the largest firecrackers producing country over world (Nirmalkar et al., 2013; Tian et al., 2014). For the Deepawali festival days in October or November, intense fireworks are happened at midnight of the Deepawali in nationwide in India, from small village areas to urban regions (Nirmalkar et al., 2013; Ambade et al., 2018). Almost every Indian family celebrates the Deepawali festival via bursting firecrackers. Massive firecracker burning event during Deepawali festival leads to deteriorating air quality as well as increasing human health risk. During fireworks emission, there is a drastic increase in aerosol mass abundance and the ambient air is also contaminated with detrimental atmospheric particulate matters (PM). The mass level of submicron particulate matters containing metals can penetrate into the deeper region of the human respiratory system. Enormous inhalable metal containing PMs are released due to firecracker burning during Deepawali festival (Godri et al., 2010; Nirmalkar et al., 2013). Throughout the Deepawali festival, the PM_{10} abundance is found to be 2–6 folds higher than the normal days (Joly et al., 2010; Segura et al., 2013). Firecrackers burning events discharge organic and inorganic matter into the air, which induces turbid atmosphere and dense clouds, the nature of which depends upon the constituents of the firecrackers. Gunpowder, KNO_3, and color producing metals like, Aluminum (Al), Calcium (Ca), Magnesium (Mg), sodium (Na), Iron (Fe) and Potassium (K) are the common constituents of firecrackers. Hence, they produce various chemical species in the atmosphere which have harmful human health effects (Vecchi et al., 2008; Liu et al., 2019). Smoke particles from the fireworks emission penetrate through the respiratory system and generate health problems like cough, fever, and dyspnoea and also cause acute eosinophilic pneumonia (Hirai et al., 2000; Barnett et al., 2005; Hamad et al., 2016).

Regular study of the size distribution of aerosols has great importance because their behavior, formation mechanism and human health effects are directly associated with the size of the tropospheric aerosols (Hillamo et al., 1988; Haywood et al., 2008; Wang et al., 2012; Remskar et al., 2015; Zhu and Wan, 2019; Nirmalkar et al., 2019). Atmospheric aerosols have three distinct modes i.e., coarse mode, droplet mode, and condensation mode. The coarse mode has a size from 2 to 50 μm, similarly, droplet mode has the size of 0.5–2 μm; whereas, condensation mode particles have 0.1–0.5 μm size. Size distribution studies not only provide information about human health implications but also, it decides the overall fate of particle into the atmosphere like long-range transportation, existence in the atmosphere, i.e., their lifetime and deposition rate to the Earth's surface (Sing et al., 2002). Earlier studies of the elemental composition of aerosols formed during such firecracker bursting events were usually focused on total suspended particles (TSP), either PM_{10} or $PM_{2.5}$ size ranges but its associated studies with metal particulate matters are very scanty.

In spite of extreme firecrackers emissions, barring a few (Godri et al., 2010; Nirmalkar et al., 2013), there are no major attempt made in the investigation of the size distribution of metals in the urban region of eastern central India. In the present work we have carried out a comparative study of size distribution of trace metals in firecracker aerosols during three different events, i.e., before Deepawali period (BDP) (October 2018), during Deepawali period (November 2018) and after Deepawali period (ADP) (December 2018) in the lower troposphere at Raipur, Chhattisgarh in the year 2018. This study presents time-series variation of coarse and fine size fractions of firework tracer metal aerosols in all three events. Probable potential penetration of particles containing metal aerosols through respiratory system and associated diseases are discussed.

2. Methods

2.1. Site description

The collection of atmospheric aerosols was done at state capital city of Chhattisgarh, namely, Raipur situated between 22°33′ N to 21°14′ N Latitude and 82°6′ to 81°38′ E Longitude (Fig. 1) throughout three different cases i.e., during fireworks emission, before fireworks emission and after fireworks emission for their comprehensive comparative study. The selected site is an urban area, which is a good representative site for firework emission.

The surrounding area is a densely populated, there are many residential communities near the Pt. Ravishankar Shukla University. Hence, it is a hotspot site for studying the firecrackers burning event. Apart from that the study site has been also used as a receptor site of pollutants by many researchers (Matawle et al., 2018; Sahu et al., 2018). The source receptor based studies suggested the greater importance of the study site. Additionally, the total area of the city is 226 km^2. The Raipur city has a population of 1.2 million as per the Census of India (2011) (Deshmukh et al., 2013). There is a National Highway, namely, Great Eastern Road that adjoins Kolkata and Mumbai, approximately 400 m away from the sampling point with frequent heavy vehicular traffic volume of nearly 25,000 vehicles per day. The study area is literally sandwiched between two industrial complexes on its eastern and western outskirts extended at distances of about 20–30 km, with some big industries such as Bhilai Steel Plant, Jamul Cement Factory, Century Cement Plant, Larson and Toubro Cement Plant, Monnet Sponge Iron and Power Plant, Woolworth Textile Plant, etc.(Deshmukh et al., 2013). It is one of the best sites to study the significant local pollutants in Raipur due to high population density and industrial or anthropogenic activities.

The aerosol collection was done at 15 m above the ground level at School of Studies in Chemistry, Pt. Raviskankar Shukla University, Raipur, which is the largest educational institute in Chhattisgarh. Raipur city has a surface area coverage of 226 Km^2 and sampling location has sea level height above of 290 m. Raipur has a semiarid climate with four distinct different seasons i.e., monsoon (June–August), post-monsoon (September–November), winter (December–February) and summer (March–May). Sampling location is under the influence of anthropogenic sources, i.e., vehicular emission, industrial pollutants, road dust, domestic emission, and emission from construction activities and biomass burning.

2.2. Size distributed aerosol sampling

Sampling was done using Anderson cascade impactor air sampler (TE 20–800, USA), which was installed on the rooftop of the sampling location as described above. The sampling of size-resolved aerosols was performed during three events i.e., BDP (October 2018, n = 5), DDP (November 2018, n = 5) and ADP (December 2018, n = 5). The sampler flow rate was set to be at 28.3 ± 0.3 $Lmin^{-1}$ to collect the atmospheric particles with 50% cutoff points as < 0.43, 0.43–0.65, 0.65–1.1, 1.1–2.1, 2.1–3.3, 3.3–4.7, 4.7–5.8, 5.8–9.0 and > 9 μm. The $PM_{>9}$ refers to the sum of stage 0 to stage 8, similarly $PM_{2.1->9}$ (Coarse Particle) refers to the sum of stage 0 to stage 3, $PM_{2.1}$ refers to the sum of stage 4 to stage 8 including back up filter (Fine Particle) and lastly $PM_{1.1}$ refers to the sum of stage 7 and stage 8 including back up filter sampler. Total 15 sets of size-resolved aerosol samples were collected on a daily basis each for 24 h. All samples were collected using pre-combusted (550 °C for 12 h) quartz fiber filters (81 mm diameter). Field blanks were collected before and after the sampling by keeping the filters onto the sampler without sucking any air.

2.3. Chemical analysis

The detailed analytical procedure for metal determination was performed according to earlier reported methods (Pervez et al., 2014). An 18 mm dia-cut of each sample collected on quartz microfiber filter was taken in a Teflon digestion vessel in which HNO_3 and H_2O_2 were added in 3:1 ratio, and was kept for microwave assisted digestion for 6–8 h. All the digested samples were diluted using ultrapure water. Barnstead Smart2pure model, Thermo Fisher was used to obtain ultrapure water (conductivity 18.2 Ω). After the digestion, samples were subjected for elemental analysis. Element (Al, Ca, K, Cu, Na, Zn, Fe, Mg) were quantified using ThermoFisher, Model iCE 3000 Atomic Absorption Spectrophotometer (AAS) associated with hydride generation and graphite furnace as atomization sources. The instrument was calibrated using the standards of the selected element. The reproducibility check was done by performing 5-replicate measurements of the samples and the relative standard deviations were found less than 5%. Field blanks were also taken and the values were subtracted from the samples. The percentage recoveries calculated to be were 103, 91, 98, 95, 110, 98 and 95% for Ca, K, Al, Cu, Fe, Na and Zn, respectively.

2.4. EC and OC analysis

An 18 mm area from the aerosol deposited filters was punched out for the estimation of OC and EC contents by DRI Thermal/Optical Carbon Analyzer (Model, 2001A) following the Interagency Monitoring of Protected Visual Environments (IMPROVE) thermal evolution protocol (Pavuluri et al., 2010). Calibration of OC-EC analyzer for carbon contents was done using a 10% sucrose solution. The analytical errors of methods were found within 5% for both OC and EC. The box blanks and field blanks were also stored and analyzed in a similar manner. An 18 mm punch of QFF was kept on a quartz tube of thermal desorption (TD) chamber of the thermal/optical analyzer and after that a stepwise temperature was programmed. In IMPROVE_A protocol the filters were heated for 120 °C, 250 °C, 450 °C, and 550 °C for OC1, OC2, OC3 and OC4 respectively, in the presence of 100% of He. However, the temperature plateau was 550 °C, 700 °C, 800 °C, and 900 °C for EC1, EC2, EC3 and EC4 respectively, in the presence of 98% He/2% O_2. The released carbon dioxide (CO_2) during the oxidation at every particulate temperature step was measured with a non-dispersive infrared detector system. The analytical errors in the triplicate analyses of the filter samples were estimated to be 5% for OC and EC both. The concentration of total carbon (TC) was calculated by summing the concentrations of OC and EC in each size fraction. As carbonate carbon (CC) also contributes to the TC in ambient aerosols, a sample aliquot was fumigated with HCl to get the peak position for CC and the correction for CC was done after verifying the thermogram.

2.5. WSOC analysis

The 16 mm quartz filter were taken in a 50 mL vial and extracted into Milli Q water by sonicating it for 15 min. Extracts were then filtered through 0.2 mm Millipore syringe filter. Before purging the extracts with pure air, in order to avoid/eliminate volatile species and inorganic carbons that may be dissolved in the extract (Deshmukh et al., 2016), the extracts were acidified with 1.2 M hydrochloric acid. Finally, the samples were analyzed for WSOC using total carbon analyzer (Shimadzu TOC-VCSH). The instrument was calibrated using potassium hydrogen phthalate. The analytical error in the measurement of WSOC was within 5% based on the triplicate analyses of the filter sample.

2.6. Estimation of inhalation dose

The extent of human exposure associated with aerosols was first calculated by Duan (1982) and Ott (1982). Many of the researchers have estimated the average exposure to find the extent of air pollutants in a certain period of time (Li et al., 2015; B. Liu et al., 2019). Another term ‘integrated exposure’ is used by many researchers to estimate the

inhalation of particles by humans. Average exposure is calculated by average concentration of air pollutants in certain time intervals. Risk exposure is then calculated by evaluating the dose of pollutant that can deposit inside human body with certain duration of time spent. The relationship between dose and exposure can be estimated by following equation:

$$D = \int C_P \times IR_{\Delta t}\, dt \quad (1)$$

Here, D indicates the inhalation dose (μg), Cp indicates the concentration of pollutants in specific time (μg m^{-3}), IRΔt represents the breathing rate of 0.027 m^3 min^{-1} (1.62 m^3 h^{-1}), the average exposure value of female and male (age range 21–51 years) as recommended by United States Environmental Protection Agency (US EPA, 2011), t is the time duration on the basis of how a person spend time (8 h) on outdoor activities (Pani et al., 2019; Mahilang and Deb, 2020).

2.7. Estimation of POC and SOC

POC and SOC were calculated using EC-tracer method (Turpin and Huntzicker, 1991) in which non-combusted OC was supposed to be negligible. Hence, minimum OC/EC ratio is considered in the POC and SOC calculation. The following equation is used:

$$POC = EC \times \left(\frac{OC}{EC}\right)_{\cdot min} \quad (2)$$

$$SOC = OC_{meas} - POC \quad (3)$$

2.8. Health risk of heavy metals

The life time average daily dose (LADD) of particular metal is the inhalation/kg of body weight/day, which has negative health impact. The non-carcinogenic effect is generally calculated in terms of hazard quotient (HQ). HQ can be obtained by dividing LAAD value to the reference dose (RfD) value which is specific for each metal (US EPA, 2001).

Following formula were used for health risk calculations:

$$LADD(mg\ kg^{-1}day^{-1}) = \frac{CM \times IR \times CF \times EF \times ED}{BW \times AT} \quad (4)$$

where, CM is the concentrations (μg m^{-3}) of metal, IR is the breathing rate (10 and 20 m^3 day^{-1} for children and adult), CF is a unit conversion factor (0.001), EF is the exposure frequency (4 days/years) and ED is the exposure duration (6 years and 24 years for children and adult) (Kong et al., 2015).

Hazardous quotient is calculated as:

$$HQ = \frac{LADD}{RfD} \quad (5)$$

where RfD is a reference dose value which is specific for each metal. The hazardous index is calculated by summing the values of HQ obtained for all metals (Kong et al., 2015; Samiksha et al., 2017).

2.9. Meteorological variables

Atmospheric variables, i.e., Temperature (T), Relative humidity (RH), Vapor pressure (VP), Wind speed (WS) and Rainfall (RF) data during entire study periods were obtained online from http://www.wunderground.com. Over the entire study period, no rainfall occurred hence RF data were excluded from the manuscript. Atmospheric variables over the entire study period are displayed in Fig. 2. The air temperature ranged from 20.0 to 28.0 °C with an average of 25.3 ± 3.30 °C. The relative humidity (RH) varied from 37 to 85% with an average of 57 ± 13%. The wind speed (WS) varied from 3 to 10 Km h^{-1} with an average speed of 5.5 ± 2.0 Km h^{-1}(North-East direction).

3. Results and discussion

3.1. Data overview

24-h average mass abundance of metals with standard deviation (SD) and range in all three events, i.e., BDP, DDP, and ADP in ultra-fine (Dp < 1.1 μm), fine mode (Dp < 2.1 μm) as well as in coarse mode (Dp > 2.1 μm) are listed in Table 1. Significantly high abundance of firework aerosol tracer metals has been observed in the present work when compared with other studies (Perrino et al., 2011; Tsai et al., 2012). Aluminum was found to be the most abundant during all the events in all size fractions and Mg was the least abundant both in ultra-fine as well as fine mode size fraction during all the events, i.e., BDP, DDP and ADP. The order of abundance of metals in ultra-fine mode size fraction during BDP, DDP and ADP were found to be Al, Fe, Ca, K, Na, Mg; Al, Zn, Cu, Fe, K, Ca, Na, Mg and Al, Zn, Cu, Fe, Ca, K, Na, Mg, respectively. The order of abundance of metals in fine mode was seen to be Al, Fe, Ca, Cu, Zn, K, Na and Mg during BDP; whereas, during DDP, metals were found in the order of Al, Cu, Zn, Fe, K, Ca, Na and Mg. Similarly, during ADP metals were obtained in the order of Al, Zn, Cu, Fe, Ca, K, Na, and Mg. In this table, it could be found that coarse mode was dominated by the metals in the order of Al > Fe > Ca > Cu > Zn > Mg > K > Na and Al > K > Zn > Fe > Cu > Ca > Mg > Na, during BDP and DDP, respectively. We have found high mass loading of metals during DDP when compared with BDP and ADP. Tandon et al. (2008) reported that some specific elements are used in the firecrackers for specific purpose like S as propellant, Cu and Fe are used as color producing agents, whereas K and Na are used as oxidizers, Mg is used as fuel and Zn is used for smoke effect etc. Moreno et al. (2007) has also reported that metal salts of K and Ca like, KNO_3 and $KClO_3$ or $KClO_4$ are used for combustion and color producing. It can be also seen from the table that abundance of all metals was highest in the fine mode over coarse mode (except Ca and K) during DDP because the burning of crackers emits freshly borne elements into the air, which causes size distribution dominated in fine mode. The metals selected as markers (Fe, Ca, Cu, Zn, K, Na and Mg) of firecrackers emission were similar to an earlier study conducted by Pervez et al. (2014). Besides the firecracker's emission, there are also possibilities of Al, Ca and Fe to come from coal ash-based cementation material, which is used in civil constructions and iron processing industries. Similarly, Al and Cu may also come from road traffic. Household solid fuel burning and kerosene burning can also emit K, which is a biomass burning tracer. Zn can be possibly originating from steel processing industries (Matawle et al., 2014). Deshmukh et al. (2017) reported the major sources of Na and Ca as sea salt and mineral dust in Raipur.

Concentration with statistical summary of carbonaceous aerosols i.e., OC, EC, TC, POC and SOC in ultra-fine, fine and coarse mode during BDP, DDP and ADP at Raipur are listed in Table 2. Interestingly, the OC, EC, TC, POC and SOC concentrations were observed to be highest during DDP in all size fractions that indicated significant enhancement in loading of carbonaceous aerosols due to extreme fireworks. The ultra-fine mode OC and EC concentrations were found in the range of 5.88–8.68 μg m^{-3} (avg 7.11 ± 1.05 μg m^{-3}) and 1.82–3.36 μg m^{-3} (avg 2.42 ± 0.76 μg m^{-3}) during BDP, 23.1–30.0 μg m^{-3} (avg 26.8 ± 2.96 μg m^{-3}) and 11.4–15.8 μg m^{-3} (avg 13.2 ± 1.92 μg m^{-3}) during DDP, 9.80–16.0 μg m^{-3} (avg 12.9 ± 2.33 μg m^{-3}) and 3.86–7.10 (avg 5.53 ± 1.41 μg m^{-3}) during ADP, respectively. The fine mode OC and EC concentration were found in the range of 6.30–9.30 μg m^{-3} (avg 7.62 ± 1.12 μg m^{-3}) and 1.95–3.60 μg m^{-3} (avg 2.59 ± 0.81 μg m^{-3}) during BDP, 24.8–32.1 μg m^{-3} (avg 28.7 ± 3.17 μg m^{-3}) and 12.2–17.0 μg m^{-3} (avg 14.2 ± 2.05 μg m^{-3}) during DDP, 10.5–17.2 μg m^{-3} (avg 13.9 ± 2.50 μg m^{-3}) and 4.13–7.60 (avg 5.93 ± 1.51 μg m^{-3}) during ADP, respectively. Similar trends were observed for coarse mode carbonaceous aerosols during BDP, DDP and ADP. The results indicated that the OC during DDP concentration was 3.5-folds and 3.7-folds

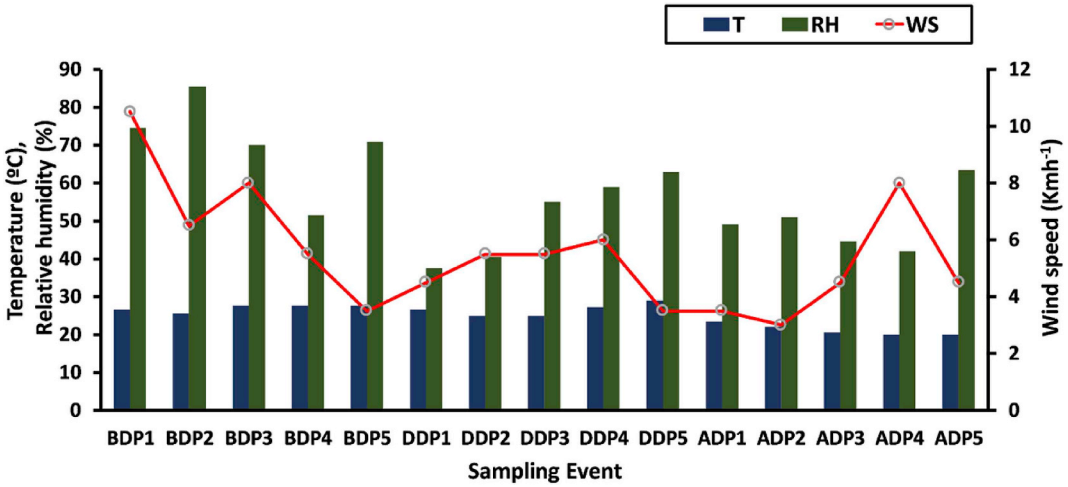

Fig. 2. Time series variation of meteorological variables (Temperature, relative humidity and wind speed) at Raipur.

Table 1
Concentration (μg m^{-3}) of aerosols measured in ultra-fine mode (Dp < 1.1 μm), fine (Dp < 2.1 μm) mode and coarse mode (Dp > 2.1 μm) in 2018 at eastern central India.

	BDP				DDP				ADP			
	[a]Ave	[b]SD	[c]Min	[d]Max	Ave	SD	Min	Max	Ave	SD	Min	Max
Ultra-fine mode												
Ca	1.38	0.44	1.63	2.78	1.95	0.32	1.42	2.38	1.67	0.36	1.34	2.25
Fe	2.08	0.12	2.83	3.12	3.28	0.15	3.08	3.52	1.70	0.13	1.52	1.91
Zn	1.11	0.18	1.71	2.25	4.49	0.47	4.03	5.37	3.82	2.01	2.32	7.80
Al	4.37	1.35	8.76	12.3	10.5	1.95	8.43	14.1	6.40	2.47	1.72	8.73
Cu	1.08	0.14	1.75	2.14	4.22	0.19	3.96	4.40	1.77	0.17	1.61	2.08
K	0.63	0.05	0.88	1.02	2.93	0.10	2.78	3.08	0.90	0.07	0.76	0.95
Mg	0.16	0.05	0.86	1.01	0.47	0.04	0.42	0.51	0.25	0.04	0.20	0.30
Na	0.36	0.02	0.25	0.29	1.52	0.13	1.39	1.75	0.68	0.02	0.65	0.71
Fine mode												
Ca	1.57	0.22	1.27	1.90	2.46	0.44	1.78	3.03	1.91	0.32	1.61	2.44
Fe	2.48	0.35	2.13	3.13	3.90	0.22	3.66	4.23	2.12	0.13	1.98	2.34
Zn	1.16	0.04	1.12	1.24	4.93	0.51	4.41	5.89	4.63	2.68	2.57	9.93
Al	4.76	1.23	2.57	6.02	13.0	1.12	11.6	14.3	9.93	0.92	8.88	11.6
Cu	1.44	0.14	1.29	1.67	5.23	0.31	4.87	5.67	2.55	0.16	2.32	2.83
K	0.78	0.14	0.53	0.91	3.46	0.11	3.27	3.60	1.27	0.14	1.03	1.39
Mg	0.20	0.04	0.13	0.24	0.59	0.03	0.54	0.63	0.37	0.03	0.32	0.42
Na	0.52	0.07	0.38	0.60	1.79	0.12	1.62	1.99	0.99	0.04	0.94	1.06
Coarse mode												
Ca	2.16	0.44	1.63	2.78	2.68	0.35	2.01	3.02	2.53	0.61	1.67	3.09
Fe	2.97	0.12	2.83	3.12	3.12	0.23	2.91	3.56	2.18	0.24	1.75	2.45
Zn	1.93	0.18	1.71	2.25	3.42	0.51	2.92	4.17	5.00	3.29	2.78	11.4
Al	10.5	1.35	8.76	12.3	11.0	1.84	8.63	13.4	8.30	3.66	1.88	12.1
Cu	1.95	0.14	1.75	2.14	2.95	0.31	2.48	3.32	2.02	0.26	1.72	2.47
K	0.93	0.05	0.88	1.02	4.42	0.33	4.11	4.84	1.06	0.09	0.93	1.17
Mg	0.94	0.05	0.86	1.01	1.40	0.08	1.32	1.55	1.19	0.15	1.06	1.44
Na	0.27	0.02	0.25	0.29	0.49	0.03	0.46	0.54	0.55	0.09	0.44	0.68

[a] Average.
[b] Standard Deviation.
[c] Minimum.
[d] Maximum.

higher than the emissions observed during normal days in ultra-fine and fine modes, respectively. Other possible sources of OC at eastern central India are both primary and secondary; primary sources include anthropogenic and natural emissions, whereas they may also form via secondary processes like heterogenic chemical reactions and gas to particles conversion (Wang et al., 2012). Similarly, significantly high abundance of EC was obtained during extreme firework days for ultra-fine (5.5-folds) and fine modes (5.4-fold) than during the normal days. However, EC can be also directly emitted from biomass burning and combustion of fossil fuels as primary aerosols in nature.

The fine mode SOC was higher than POC during DDP, indicating secondary formation as prominent source of carbonaceous aerosols. The DDP period was observed to have high concentration of fine mode POC. Gaseous pollutants emitted from fireworks events could be responsible for triggering the significant secondary formation in atmosphere of eastern central India. SOC was found to be high during DDP that must be due to secondary formation and gas to particles conversion, and further the fine mode particles were converted to coarse mode by agglomeration. Fine mode POC, WSOC, and SOC were found higher compared to ultra-fine and coarse modes during DDP, ADP and BDP, respectively. Generally, burning activities release gases that condense over fine particles, as fine particles have larger surface area, which can

Table 2
Statistical summary of carbonaceous aerosols in ultra-fine, fine and coarse mode of aerosols at eastern central India.

	BDP				DDP				ADP			
	Avg	Sd	Min	Max	Avg	Sd	Min	Max	Avg	Sd	Min	Max
Ultra-fine mode												
OC	7.11	1.05	5.88	8.68	26.8	2.96	23.1	30.0	12.9	2.33	9.80	16.0
EC	2.42	0.76	1.82	3.36	13.2	1.92	11.4	15.8	5.53	1.41	3.86	7.10
WSOC	2.39	0.21	2.15	2.68	13.0	2.57	10.1	15.6	3.52	0.35	2.91	3.74
WSOC/OC	0.34	0.02	0.31	0.37	0.48	0.06	0.41	0.53	0.27	0.03	0.23	0.30
OC/EC	3.08	0.66	2.35	3.94	2.06	0.37	1.60	2.59	2.41	0.50	2.09	3.29
TC	9.53	1.71	7.84	12.0	40.0	3.63	36.8	45.8	18.5	3.54	14.3	23.1
POC	2.21	0.33	1.83	2.70	7.40	0.82	6.39	8.29	6.34	1.14	4.80	7.85
SOC	4.90	0.72	4.06	5.99	19.4	2.15	16.7	21.7	6.60	1.19	5.00	8.17
Fine mode												
OC	7.62	1.12	6.30	9.30	28.7	3.17	24.8	32.1	13.9	2.50	10.5	17.2
EC	2.59	0.81	1.95	3.60	14.2	2.05	12.2	17.0	5.93	1.51	4.13	7.60
WSOC	2.43	0.82	1.96	3.88	19.6	3.52	16.4	25.6	6.55	1.56	5.18	9.09
WSOC/OC	0.32	0.05	0.30	0.42	0.68	0.10	0.54	0.80	0.47	0.04	0.41	0.53
OC/EC	3.08	0.66	2.35	3.94	2.06	0.37	1.60	2.59	2.41	0.50	2.09	3.29
TC	10.2	1.83	8.40	12.9	42.9	3.89	39.5	49.1	19.8	3.79	15.3	24.8
POC	2.37	0.35	1.96	2.89	7.93	0.88	6.84	8.88	6.79	1.23	5.15	8.41
SOC	5.25	0.78	4.34	6.41	20.8	2.30	17.9	23.3	7.07	1.28	5.36	8.75
Coarse mode												
OC	5.08	0.75	4.20	6.20	19.1	2.12	16.5	21.4	9.24	1.67	7.00	11.4
EC	1.73	0.54	1.30	2.40	9.45	1.37	8.12	11.3	3.95	1.00	2.76	5.07
WSOC	2.39	0.21	2.15	2.68	13.0	2.57	10.1	15.6	3.52	0.35	2.91	3.74
WSOC/OC	0.47	0.05	0.42	0.52	0.68	0.10	0.57	0.87	0.38	0.04	0.33	0.42
OC/EC	3.08	0.66	2.35	3.94	2.06	0.37	1.60	2.59	2.41	0.50	2.09	3.29
TC	6.81	1.22	5.60	8.60	28.6	2.59	26.3	32.7	13.2	2.53	10.2	16.5
POC	1.58	0.23	1.31	1.93	5.29	0.59	4.56	5.92	4.53	0.82	3.43	5.61
SOC	3.50	0.52	2.90	4.28	13.9	1.53	12.0	15.5	4.71	0.85	3.57	5.84

provide suitable conditions for condensation of aerosols (Engling et al., 2009; Levin et al., 2010; Li et al., 2019). Nirmalkar et al. (2013) have reported that the ultra-fine aerosol particles with 0.1–0.5 μm size released through biomass burning process condense over fine particles to grow coarse particles sequentially under suitable meteorological conditions.

During DDP, fine mode OC and EC were dominated over coarse mode OC and EC, respectively. The coarse mode loading is also significant because of prevailed meteorology offering more suitable conditions for secondary formation by accelerating the heterogeneous reactions in aerosols, which results in the formation of coarse particles onto pre-existed aerosols (Huang et al., 2006). The POC concentration was dominated in coarse mode over fine mode during entire study period. Besides the firecracker's emissions, EC and POC both may come from primary emissions and such loading with significant contribution of WSOC in coarse mode indicates that the study site is under the influence of significant burning emissions, i.e., biomass burning. Fine mode WSOC concentration was found to be higher during DDP followed by BDP and ADP. Wang et al. (2012) have reported that WSOC are mainly from secondary formation and biomass burning processes. The significant loading of WSOC, in the present work, over entire study period also indicated that the aerosols from secondary formation and biomass burning including fireworks emission could be the dominant sources in eastern central India.

3.2. Size distribution of aerosols

Size distribution of metal aerosols in all three events, i.e., BDP, DDP, and ADP over nine different size fractions are shown in Fig. 3(a–l) and 4 (a-l). A bimodal size distribution with peaks at 0.43–1.1 μm and 4.7–9.0 μm was found, with fine mode dominance for Cu and Al indicating DDP event was strongly influenced from burning emission, i.e., fireworks. The single fine mode peak in DDP indicates that Cu and Al were contributed from firecrackers since Cu and Al are used in firecrackers as color producing agents (Baptista et al., 2008). Earlier studies have reported that the general sources of Cu are diesel engine and unleaded gasoline. Besides these, Cu also comes from Cu-containing fungicides, metalworking factories and electroplating materials (Nriagu and Pacyna, 1998; Baptista et al., 2008).

Size distribution of Zn was bimodal with equally intense peaks at 0.43–1.1 μm μm in fine mode and at 4.7–9.0 μm in coarse mode during DDP and an intense coarse mode peak at 4.7–9.0 μm during BDP and ADP. Matawle et al. (2014) have reported that the dominant sources of Zn in Raipur are steel manufacturing and galvanizing industries. However, during DDP, the dominance of firecracker's emission over other sources could be the reason of getting equally intense peaks both in coarse and fine modes.

For Fe and Ca, the bimodal size distribution with dominance in coarse mode (4.7–9.0 μm) over fine mode (0.43–1.1 μm) suggested two different sources of metals in Raipur aerosol. Aksu (2015) has reported the contamination of atmosphere from Fe by anthropogenic source, i.e., emissions through iron processing industries. Deshmukh and coworkers (2017) have reported that the two main sources of atmospheric Ca are mineral dust and sea salt. Here, the fine mode peak during DDP in our study is possibly due to the extreme firecrackers burning and the coarse mode peak is due to absorption of gaseous precursors and particles over the surface of mineral dusts.

In case of Mg, there was a bimodal size distribution with a peak in fine mode (0.43–1.1 μm) and a peak in coarse mode (4.7–9 μm) obtained for BDP, DDP and ADP. Similar size distribution of Mg was reported in eastern central India by Verma et al. (2010). They reported that the contribution of sea salt to Mg loading was negligible and the only dominated source of Mg was mineral dusts. Whereas another modeling study done at Raipur has reported different sources of Mg influencing the atmospheric aerosols along with natural sources. Matawle et al. (2014) have found some anthropogenic sources, i.e., road traffic, household solid fuel burning, and steel processing industries significantly contributing to total Mg loading in PM. Hence, the reason for coarse mode Mg in our study is from the mixture of sources during ADP and BDP, whereas the fine mode peak of Mg is probably due to firecrackers emission because Mg is used as fuel for firecrackers that contributed to fine mode particles during DDP.

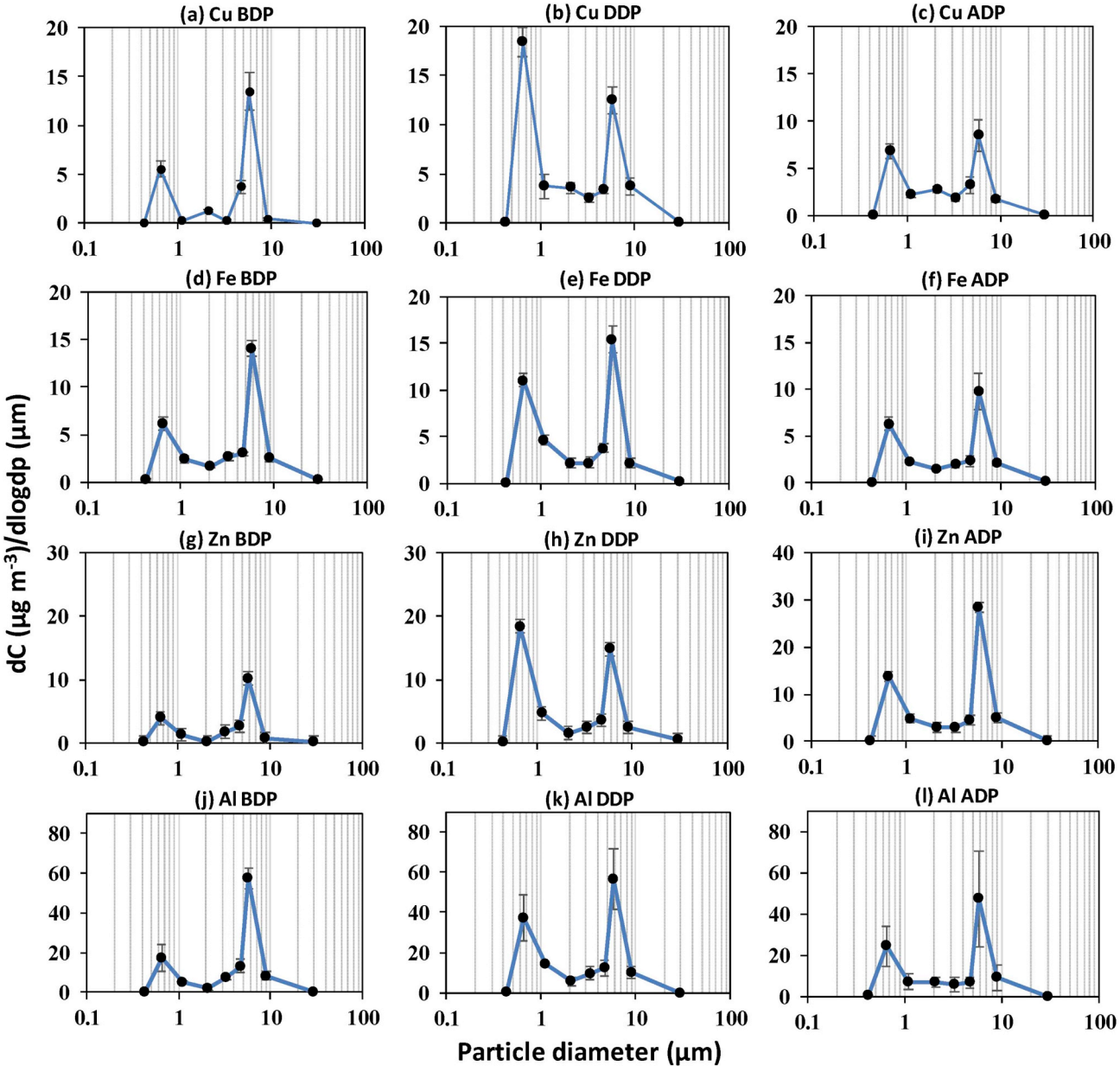

Fig. 3. Size distribution of Cu, Fe, Zn and Al during BDP, DDP and ADP at Raipur.

Fig. 4 shows that the size distribution of Na is bimodal during BDP, DDP and ADP with peaks at coarse mode (4.7–9 µm) and fine mode (0.43–1.1 µm). During the DDP, comparatively more intense peak at fine mode (0.43–1.1 µm) indicates the high burning activities and fine particles emission. For Na, a dominated peak at coarse mode is previously observed in Raipur potentially due to sea salt and mineral dust from soil dust resuspension (Deshmukh et al., 2017). However, during DDP, fine mode peak appeared for Na was possibly due to extreme firecrackers burning because Na is used commonly in the firecrackers as oxidizer (Pervez et al., 2014).

For K, a bimodal size distribution with coarse mode peak at 4.7–9 µm and fine mode peak at 0.43–1.1 µm were found for all the three events but interestingly DDP event had an intense peak in fine mode at 0.43–1.1 µm size. Whereas coarse mode dominated peak at 4.7–9 µm size range was observed in the other two events. This indicated that there must be different sources which were also influencing the air mass during DDP. During DDP intense peak in fine mode was due to the mixture of two major sources, namely, firecrackers emission and biomass burning activities. Yamasoe et al. (2000) have also found bimodal size distribution of K with fine mode peak reported was due to biomass burning and coarse mode peak reported was due to mineral dust and sea salt. The possible sources of coarse mode K was reported to be sea salts and soil dust particles (Huang et al., 2012). The K derived from firecrackers emission is mostly enriched in fine mode, however, possibilities of K from firecrackers towards the coarse mode is less significant. Because firecrackers mostly release gaseous species and freshly borne fine particles in the atmosphere. Deshmukh et al. (2017, 2016) reported the fine mode peak of K from biomass burning and coarse mode peak was due to soil dust particle and sea salts at Raipur aerosols. Based on the strong correlation of K with other sea salt and mineral dusts derived species they reported sea salt and dusts particles as source for significant coarse mode peak of K. They also conducted air mass trajectory analysis to find the possible transported ways of sea salt derived K at Raipur.

Fig. 5 shows the size distribution of EC, OC and WSOC during BDP, DDP and ADP at Raipur. A bimodal size distribution of OC (a dominated coarse mode peak at 3.3–4.7 µm and fine mode peak at 0.65–1.1 µm) was found over the entire period. The concentrations in each size

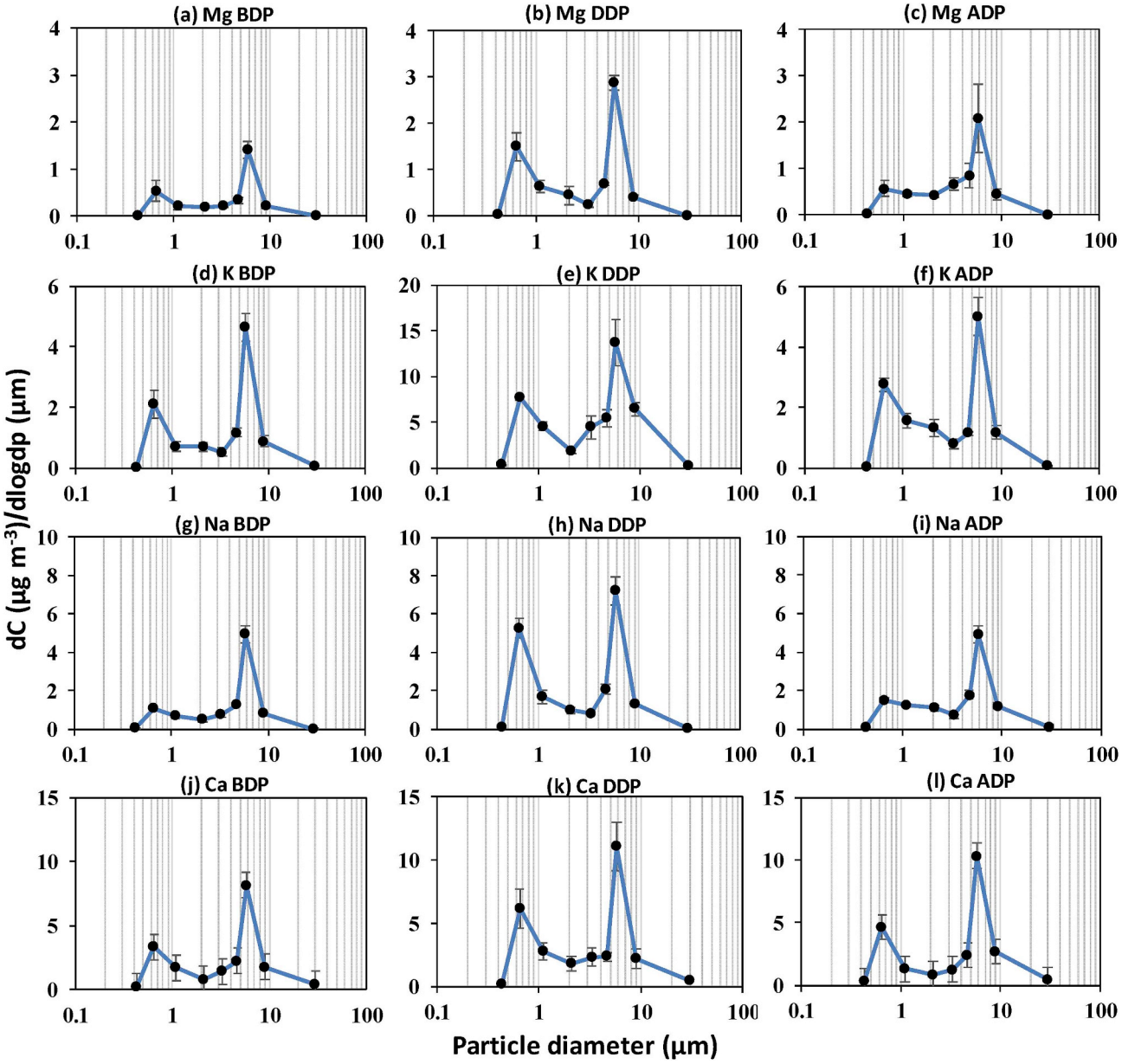

Fig. 4. Size distribution of Mg, K, Na and Ca during BDP, DDP and ADP at Raipur.

fractions were highly enhanced during extreme firework period. Similar size distribution was found by Deshmukh et al. (2017) in which highly oxidized water-soluble organic aerosols formation from biomass burning was reported as dominant source of fine mode aerosols at Raipur. Similarly, a bimodal size distribution of EC was obtained during BDP, DDP and ADP periods. The fine mode dominated peak at 0.65–1.1 µm of EC was found in all the different study periods. The reason could be due to the primary emission from combustion sources. Kong et al. (2015) have also reported high EC loading during extreme firework days in China.

The carbonaceous aerosols (EC, OC and WSOC) exhibited a large deviation of the concentration in all size fractions, during BDP, ADP and DDP event (Fig. 6). The OC itself contains many fractions like POC, SOC, and WSOC (Tang et al., 2016). The carbonaceous aerosols are derived from diverse sources. The atmospheric variables like, relative humidity, ambient temperature, wind speed and boundary layer dynamics also play significant role towards the total OC loading (Jurado et al., 2008; Nirmalkar et al., 2020). Apart from the emission sources and their emission strength, the atmospheric variables are major causes that control the size distribution of carbonaceous aerosols. The SOC formation during the aging process is also significant at Raipur. Hence, the extent of POC and SOC along with atmospheric variables could be the reason for large deviation in the carbonaceous aerosols loading at urban area of Raipur. In addition, firecrackers burning activities and their delayed effect could add a significant carbonaceous component in the troposphere during DDP and ADP. Hence, it can be concluded that the dynamics of boundary layers, atmospheric variables, diverse sources and their emission strength, SOA formation and atmospheric aging were the possible reasons for large deviation in the size distribution of carbonaceous aerosols.

WSOC are mainly produced from primary emission and from secondary organic aerosols formation process through gas phase oxidation of VOC in troposphere. WSOC like levoglucosan and mannosan are highly water-soluble species produced from biomass burning activities (Fu et al., 2010). In the present work, coarse mode peak for WSOC was significantly high in comparison to fine mode because coarse mode WSOC are formed via aggregation or heterogenous reaction of primary aerosols in the particles phase (Miyazaki et al., 2011). The smaller

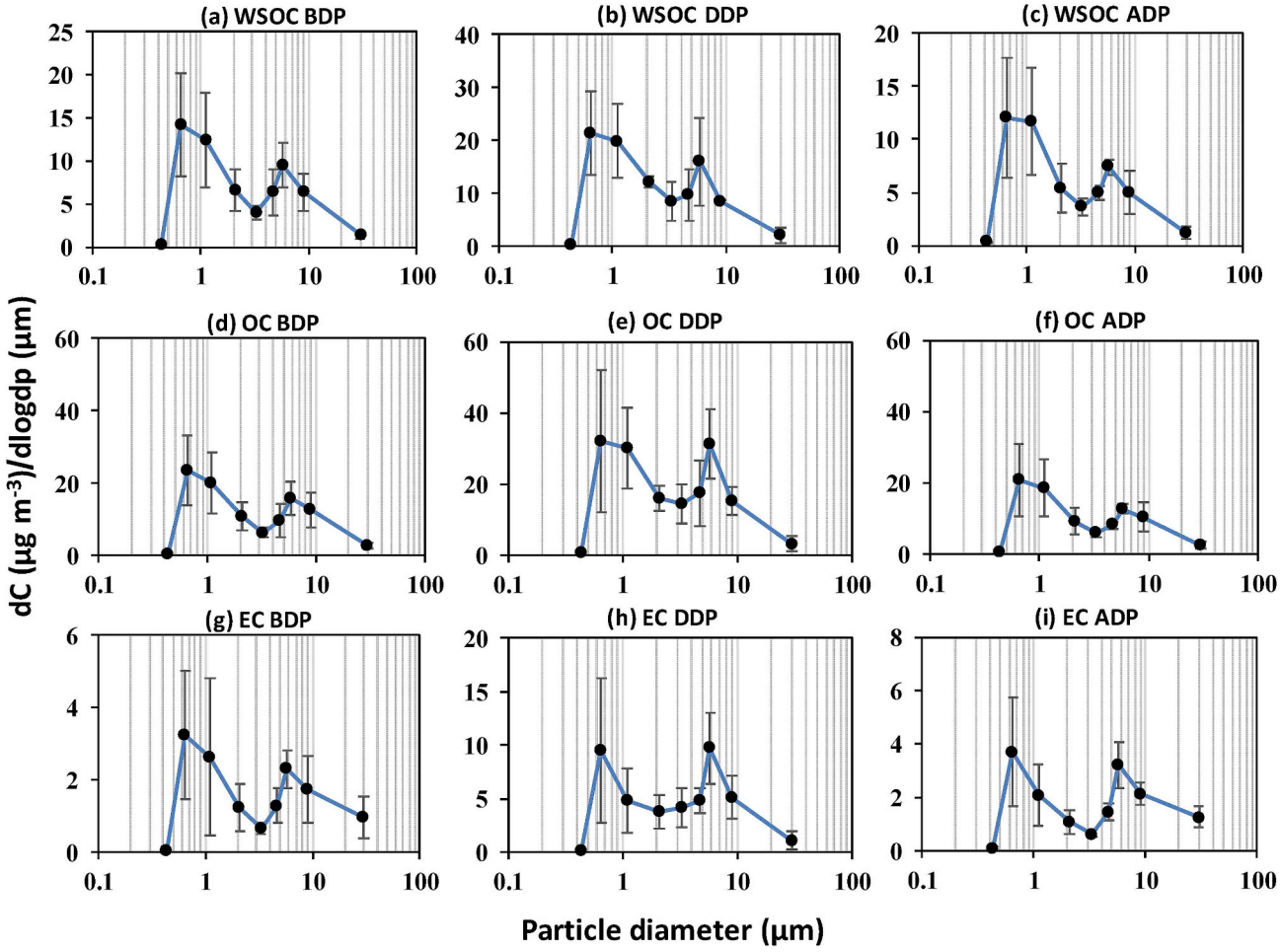

Fig. 5. Size distribution of WSOC, EC and OC during BDP, DDP and ADP period at Raipur.

particles having large surface area provide more exposure to chemical reactions that triggers aging to form the coarse particles (Kanakidou et al., 2005). In the present investigation, gaseous pollutants from firecrackers burning could be the reason for significant secondary formation that contributes to WSOC fraction of carbonaceous aerosols.

3.3. Metal-metal correlation

Pearson correlation of metal aerosols in between fine size fractions in all three events, i.e., BDP, DDP, and ADP, are listed in Table 3. Strong correlation ($r^2 \geq 0.5$) indicates similar source and negative or weak correlation ($r^2 \leq 0.5$) indicates diverse sources of metals aerosols. K and Cu were well correlated with each other with $r^2 = 0.57$. Similarly,

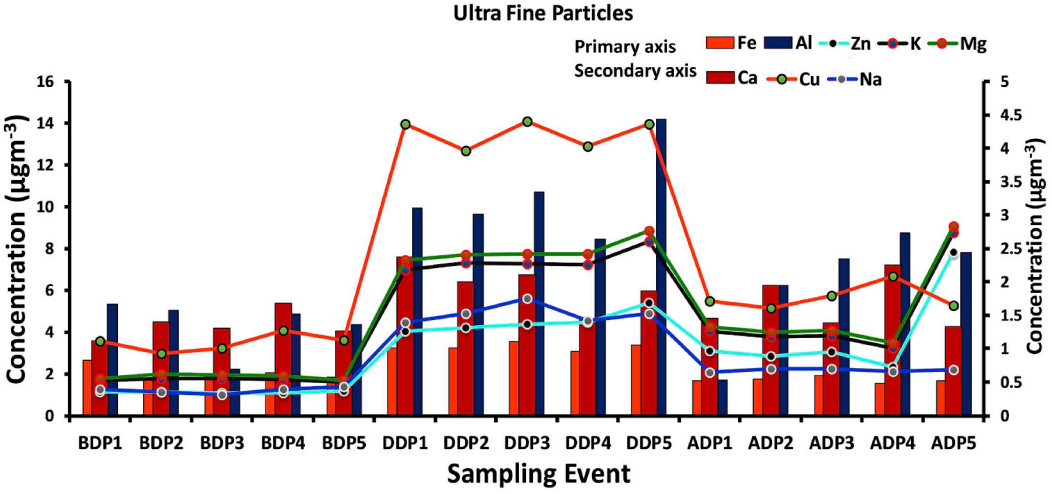

Fig. 6. Time series variation of metals associated (different coloured lines and bars represent different metals concentrations) in ultra-fine particles of firecracker aerosols tracer metals at Raipur.

Table 3
Pearson correlation of firecrackers emission tracer metals during BDP, DDP and ADP at eastern central India.

	Ca	Fe	Zn	Al	Cu	K	Mg
BDP							
Fe	−0.56[b]						
Zn	−0.44[b]	−0.38					
AL	−0.07	0.33	−0.36				
Cu	0.27	0.43[b]	−0.36	0.31			
K	0.65[a]	−0.02	−0.85[a]	−0.10	0.06		
Mg	0.67[a]	−0.26	−0.66[a]	−0.29	−0.18	0.95[a]	
Na	−0.09	0.08	0.23	0.69[a]	0.53[b]	−0.60[a]	−0.73[a]
DDP							
Fe	0.01						
Zn	−0.59	0.53[a]					
Al	0.35	0.87[a]	0.36				
Cu	0.50[b]	0.82[a]	0.11	0.96[a]			
K	0.94[a]	0.13	−0.29	0.51[b]	0.57[b]		
Mg	−0.45	−0.55	0.28	−0.71[a]	−0.84	−0.38	
Na	−0.11	0.77[a]	0.27	0.41[b]	0.44[b]	−0.18	−0.27
ADP							
Fe	−0.45[a]						
Zn	−0.58[b]	−0.16					
Al	−0.32	−0.39	0.86[a]				
Cu	0.44[b]	−0.57[b]	−0.14	0.39			
K	0.02	−0.68	0.35	0.16	−0.21		
Mg	0.42[b]	−0.40	0.35	0.64[a]	0.57[b]	−0.12	
Na	−0.40[b]	0.92[a]	−0.42	−0.59[b]	−0.44	−0.66[a]	−0.64[a]

[a] Correlation is significant at 0.01 level.
[b] Correlation is significant at 0.05 level.

a significantly strong correlation was found between Mg and K (r^2 = 0.95) during BDP. Na is well correlated with Cu (r^2 = 0.52) and Al (r^2 = 0.68), whereas either weak or negative correlation between other metals during BDP in fine mode were found. The strong correlation between K and Ca, suggested a similar source of origin, i.e., emission from cementation or civil construction works. Whereas a strong positive correlation found between Mg and K was possibly due to dominance of biomass burning. During DDP Al was well correlated with Fe (r^2 = 0.87) and Cu (r^2 = 0.96). Strong correlations were found between Zn and Al (r^2 = 0.53), Cu and Fe (r^2 = 0.82), and Cu and Ca (r^2 = 0.49). The reason behind such strong correlations could be attributed to the use of a mixture of these metals' salts, to illuminate with different colors on burning, during manufacturing of firecrackers. During ADP, Cu was fairly correlated with Ca (r^2 = 0.44), Zn was strongly correlated with Al (r^2 = 0.85). Similarly, Mg was strongly correlated with Ca (r^2 = 0.42), Al (r^2 = 0.644) and Cu (r^2 = 0.56). Such correlations were found possibly due to emission of these metals from similar sources, i.e., cementation or construction activities from nearby areas (Matawle et al., 2014). However, all other metals were weakly or negatively correlated with each other during this event indicating diverse sources. A strong correlation between Na and Fe was found common in all the events, whereas the correlations between Na with Al and Cu with Fe were found common in BDP and DDP, which indicated that a common source has also affected all of the events.

3.4. Time series variation

Time series variations of ultra-fine, fine and coarse particles during all the events in 2018 are displayed in Figs. 6–8. Higher abundances of fireworks tracer metals in ultra-fine, fine and coarse particles observed during DDP were mainly due to the burning of the enormous number of firecrackers in this festival. It could be observed from the figure that all the DDP events have high loading compared to BDP and ADP. During DDP bursting firecrackers had led to an increase in fine particles over coarse particles. During DDP, all coarse particles had high loading over other events because of the particle's growth. It has been reported that fine particles can accumulate or condense together to form coarse particles (Pandey et al., 2012). Similar variation trends towards increase and decrease in concentration of metals were found among the pairs, Fe–Al and Na–Zn during DDP only. This indicated the dominance of similar sources of variation during Deepawali period. The variation trends of Mg–K were found common over entire study period but an overall high loading was found only during DDP. This indicated the dominance of biomass burning during the entire study period with fireworks as an additional source during DDP.

3.5. Atmospheric aging of particles

Earlier studies reported so far were focused on the short-term influence of fireworks on air quality (Jing et al., 2014). However, no significant attempts were made on the atmospheric aging associated with fireworks particles in ultra-fine, fine and coarse size fractions. It is emphasized that during DDP period the contribution of anthropogenic sources other than the fireworks emissions were less, so the atmosphere during DDP period days was mainly influenced from the significant contribution of fireworks, atmospheric aging processes, dispersion, deposition and transformations of particles. Sarkar et al. (2010) have reported that the primary pollutants like NO_x, SO_2 etc. emitted during fireworks may act as oxidizer to form secondary organic and inorganic aerosols or may get adsorbed on pre-existed aerosols particles. Significantly high WSOC/OC ratio was observed during DDP (Table 2) events indicated high loading of atmospherically aged particles in firework days. Low wind speed and lower boundary layer height facilitates trapping the gaseous pollutants near ground level, and high relative humidity triggers the formation of SOA that further condenses over pre-existing aerosols (Sotiropoulou et al., 2006). This could be the reason for significant coarse mode loading of aerosols suggesting occurrence of atmospheric aerosols aging in eastern central India during DDP. Many of the other works have reported the significant secondary formation of NH_4^+, NO_3^- and SO_4^{2-} from gases released from fireworks burning (Wang et al., 2007; Yang et al., 2014). Do et al. (2012) reported that soot-EC is directly emitted from fireworks. They have found strong correlation between NO_3^- (r^2 = 0.47) and SO_4^{2-} (r^2 = 0.56) indicating that both of these chemical species adhere on to soot particles. In another work OC/EC ratio of 6.8 was reported during fireworks in Chinese New Year festival, which was reported to be due to the high enrichment of OC1, OC2 and OPC. All carbonaceous fractions are related to volatile nature of organic matters used for firecrackers production. The reported smelting points of ploxyxethylene, polyvinyl alcohol and shell-lac were 212, 230 and 115–120 °C, respectively, and all these temperatures were less than the detecting temperature of OC2 fraction, i.e., 230 °C (Zhang et al., 2013). Accordingly, in our work too, these carbonaceous aerosols fractions (OC1 and OC2) were directly emitted to the atmosphere from fireworks. It is quite interesting to note that although aging process includes the coarse particles formation which have relatively lower health risks compared to fine particles, but the aged particles are highly contaminated with metals, carbonaceous aerosols and secondary organic aerosols which can cause high health risks.

3.6. Health problems associated with aerosols

In recent years, air quality and public health have become one of the most emerging issues due to a wide variety of chemical constituents and different size of particulate matters (PMs) released from a variety of sources into the atmosphere (Castro et al., 2015). UNICEF (2016) has published a report in which they mentioned that in developing countries approximately 0.6 million children die every year due to inadequate air quality. A study conducted in China found mortality rates of 0.36 and 0.42% due to cardiovascular and respiratory diseases, respectively (Lu et al., 2015).

Inhalation dose of EC is calculated to study the influence of EC on human health. The results of calculated inhalation dose of EC in eastern

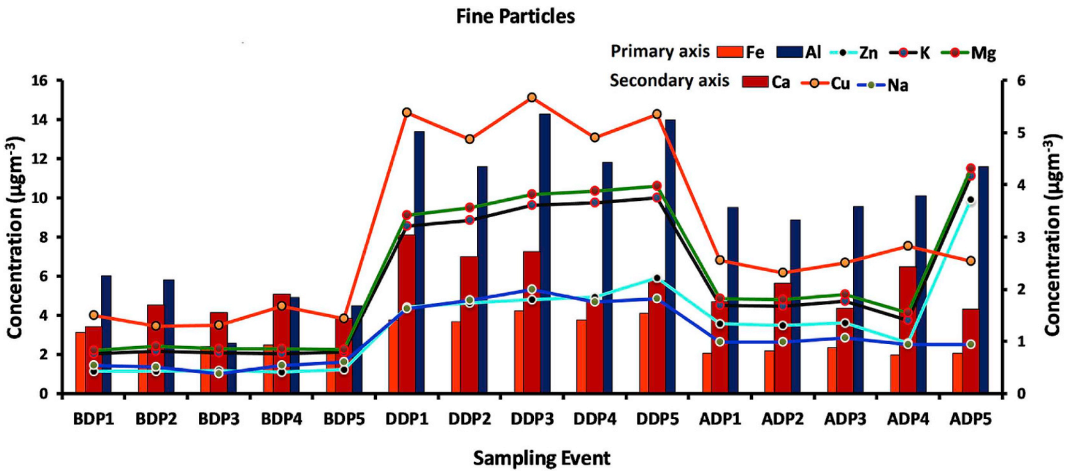

Fig. 7. Time series variation of metals associated (different coloured lines and bars represent different metals concentrations) in fine particles of firecracker aerosols tracer metals at Raipur.

central India during ADP, BDP and DDP are listed in Table 4. The calculated dose in this work was found significantly high during DDP over ADP and BDP period that could cause severe respiratory diseases in humans. There is, therefore, a strong need of attention to protect human health. An earlier work carried out during 2007–2013 has reported that increase in detrimental pollutants present in air can cause increase in daily hospital visit due to respiratory disease (Pongpiachan and Paowa, 2015). High values of inhalation dose of EC were obtained during DDP for ultra fine mode, fine mode and coarse mode with average values of 65.2(± 18.2), 87.6(± 74.5) and 44.7(± 17.3) m^3 h^{-1}, respectively. This indicated the high health risk of EC in extreme firecrackers burning days. The inhalation dose of EC was found highest in fine mode over ultrafine mode and coarse mode. Also, lowest dose was observed during BDP period in coarse, fine and ultrafine mode aerosols.

The potential health impact and non-carcinogenic risk of human exposure with metal present in ultrafine mode, fine mode and coarse mode were assessed in the aerosol samples of Raipur. Health risk was measured by the calculating the LADD, HQ and HI values (described in section 2.8). Table 6 and Table 7 shows the non-carcinogenic risk assessment, calculated for adult and children during ADP, DDP and ADP period. The high HQ values were obtained during DDP season for all four (Fe, Zn, Cu, and Al) metals in all size fractions. HI values (in ultra-fine, fine and coarse mode) for adults were also calculated to be less than 1 during BDP (1.19E-04, 1.51E-04 and 2.19E-04), DDP (4.25E-04, 5.19E-04 and 3.15E-04) and ADP (2.06E-04, 2.89E-04 and 2.46E-04) period, respectively. HI values for children (in ultra-fine, fine and coarse mode) were also found to be less than 1 during BDP (1.19E-04, 1.51E-04 and 2.19E-04), DDP (4.25E-04, 5.19E-04 and 3.15E-04) and ADP (2.06E-04, 2.89E-04 and 2.46E-04), respectively. HI value 1 or greater than 1 is indication of potential health risk (Kong et al., 2015; Samiksha et al., 2017). However, in this study the risk exposure of metals was found insignificant.

The calculated average abundances of metals during ADP, DDP, and BDP, along with ultra-fine, fine and coarse particles are separately displayed in the pie chart (Fig. 9). The average abundances of fine and ultrafine particles during DDP were found highest followed by ADP and BDP due to the emission of fresh airborne particles from extreme firecrackers burning. In addition, coarse particles abundance during DDP was also found highest over ADP and BDP. The reason possibly may be the growth of the fine particles because they can condense together and form larger particles. Fine particles can enter lower respiratory tract, i.e., trachea and alveoli, so they are more harmful than the coarse particles.

Apart from high loading DDP period, the concentrations of metals and carbonaceous aerosols were also found higher during ADP than BDP in all size fractions. This should be due to the delayed effect of atmospheric aerosols. Aerosols emitted from the firecrackers can last long in the troposphere. It could be condensed over the particles phase and present in over particle during aging process. Similarly, Kong et al. (2015) also reported that the long existence of firecrackers derived

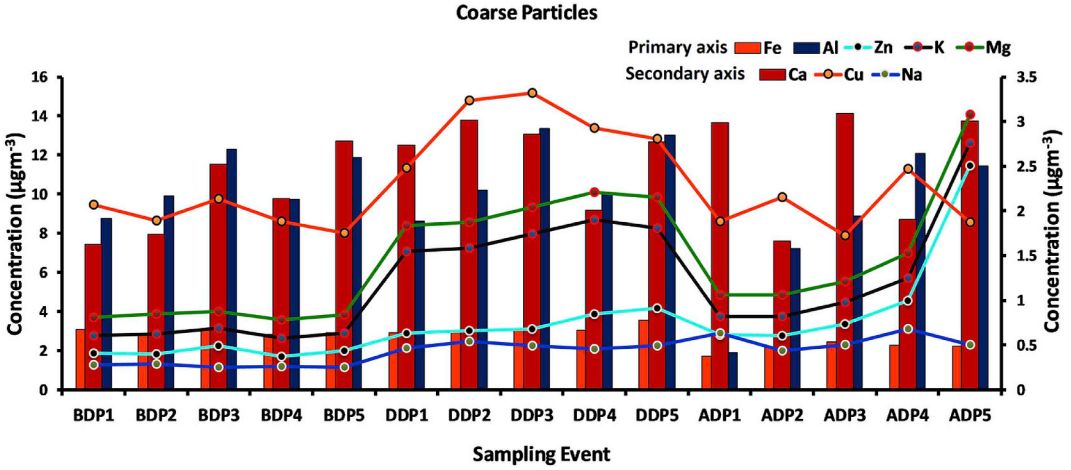

Fig. 8. Time series variation of metals associated (different coloured lines and bars represent different metals concentrations) with coarse particles of firecracker aerosols tracers' metals at Raipur.

Table 4
Inhalation dose of elemental carbon in ultra-fine, fine and coarse mode of aerosols.

	BDP				DDP				ADP			
	Avg	Sd	Min	Max	Avg	Sd	Min	Max	Avg	Sd	Min	Max
Ultra-fine mode EC	23.1	8.2	10.8	33.2	65.2	18.2	45.1	91.3	71.7	18.2	50.0	92.0
Fine Mode EC	31.0	7.7	25.3	43.4	87.6	74.5	42.8	220	76.8	19.5	53.6	98.5
Coarse mode EC	22.4	7.0	16.8	31.1	44.7	17.3	27.5	68.7	51.2	17.7	26.8	76.4

Table 5
Concentration (μg m^{-3}) of firework aerosols tracer metals from different literatures.

S.N.	Event	Study site	Particles Size	Tracer metal concentration (μg m^{-3})							References
				Cu	Zn	Fe	Na	Ca	K	Al	
1.	Deepawali Festival	Tezpur, India	PM_{10}	0.02	NA[a]	NA	0.00	0.00	0.00	NA	Deka and Hoque (2014)
2.	Chinese Spring Festival	Nanjing, China	$PM_{2.5}$	0.08	0.09	0.80	0.42	0.36	3.33	0.80	Kong et al. (2015)
3.	Sant Joan fireworks event	Parc Migdia	$PM_{2.5}$	0.02	0.07	NA	0.20	0.20	2.60	NA[a]	Moreno et al. (2010)
4.	Sant Joan fireworks event	Escola Musica	$PM_{2.5}$	0.01	0.08	NA	0.30	0.30	1.30	NA	Moreno et al. (2010)
5.	Firework Festival in Yanshui	Tainan, Taiwan	PM_{10}	0.00	0.03	0.15	0.54	0.16	0.22	0.20	Do et al. (2012)
6.	New Year Mexico	Mexico	NA	NA	NA	NA	0.10	0.30	0.80	NA	Retama et al. (2019)
7.	New Year's Eve	United States of America	$PM_{2.5}$	0.30	NA	0.38	NA	0.52	NA	NA	Liu et al. (2019)
8.	Chinese New Year	China	$PM_{2.5}$	0.04	NA	0.27	NA	0.31	NA	NA	Liu et al. (2019)
9.	Yuan Xiao Festival	China	$PM_{2.5}$	0.14	NA	0.82	NA	0.13	NA	NA	Liu et al. (2019)
10.	Deepawali	Raipur, India	Coarse	2.68	3.42	3.12	0.49	2.68	4.42	11.0	**Present Study**
11.	Deepawali	Raipur, India	Fine	5.23	4.93	3.90	1.79	2.46	3.46	13.0	**Present Study**

[a] Not available.

Table 6
Non-carcinogenic risks due to human exposure (adults) with metals during BDP, DDP and ADP period.

	BDP		DDP		ADP	
	LADD[a]	HQ[b]	LADD	HQ	LADD	HQ
Ultra-fine mode						
Fe	6.51E-06	9.30E-06	1.03E-05	1.47E-05	5.32E-06	7.60E-06
Zn	3.48E-06	1.16E-05	1.41E-05	4.69E-05	1.20E-05	3.99E-05
Al	1.37E-05	1.37E-05	3.29E-05	3.29E-05	2.00E-05	2.00E-05
Cu	3.38E-06	8.45E-05	1.32E-05	3.30E-04	5.54E-06	1.39E-04
HI[c]		**1.19E-04**		**4.25E-04**		**2.06E-04**
Fine mode						
Fe	7.77E-06	1.11E-05	1.22E-05	1.74E-05	6.64E-06	9.48E-06
Zn	3.63E-06	1.21E-05	1.54E-05	5.15E-05	1.45E-05	4.83E-05
Al	1.49E-05	1.49E-05	4.07E-05	4.07E-05	3.11E-05	3.11E-05
Cu	4.51E-06	1.13E-04	1.64E-05	4.09E-04	7.98E-06	2.00E-04
HI		**1.51E-04**		**5.19E-04**		**2.89E-04**
Coarse						
Fe	9.30E-06	1.33E-05	9.77E-06	1.4E-05	6.83E-06	9.75E-06
Zn	6.04E-06	2.01E-05	1.07E-05	3.57E-05	1.57E-05	5.22E-05
Al	3.29E-05	3.29E-05	3.44E-05	3.44E-05	2.60E-05	2.60E-05
Cu	6.11E-06	0.000153	9.24E-06	2.31E-04	6.32E-06	1.58E-04
HI		**2.19E-04**		**3.15E-04**		**2.46E-04**

[a] Life time average daily dose.
[b] Hazard quotient = LadD/RfD.
[c] Hazardous Index.

Table 7
Non-carcinogenic risks due to human exposure (children) with metals during BDP, DDP and ADP period.

Metals	BDP		DDP		ADP	
	LADD[a]	HQ[b]	LADD	HQ	LADD	HQ
Ultra-fine mode						
Fe	2.89E-06	4.12E-06	4.55E-06	6.50E-06	2.36E-06	3.37E-06
Zn	1.54E-06	5.14E-06	6.23E-06	2.08E-05	5.3E-06	1.77E-05
Al	6.07E-06	6.07E-06	1.46E-05	1.46E-05	8.88E-06	8.88E-06
Cu	1.50E-06	3.75E-05	5.86E-06	1.46E-04	2.46E-06	6.14E-05
HI[c]		**1.19E-04**		**4.25E-04**		**2.06E-04**
Fine mode						
Fe	3.44E-06	4.92E-06	5.41E-06	7.73E-06	2.94E-06	4.20E-06
Zn	1.61E-06	5.37E-06	6.84E-06	2.28E-05	6.43E-06	2.14E-05
Al	6.61E-06	6.61E-06	1.80E-05	1.80E-05	1.38E-05	1.38E-05
Cu	2.00E-06	5.00E-05	7.26E-06	1.81E-04	3.54E-06	8.85E-05
HI		**1.51E-04**		**5.19E-04**		**2.89E-04**
Coarse mode						
Fe	4.12E-06	5.89E-06	4.33E-06	6.19E-06	3.03E-06	4.32E-06
Zn	2.68E-06	8.93E-06	4.75E-06	1.58E-05	6.94E-06	2.31E-05
Al	1.46E-05	1.46E-05	1.53E-05	1.53E-05	1.15E-05	1.15E-05
Cu	2.71E-06	6.77E-05	4.09E-06	1.02E-04	2.80E-06	7.01E-05
HI		**2.19E-04**		**3.15E-04**		**2.46E-04**

[a] Life time average daily dose.
[b] Hazard quotient = LadD/RfD.
[c] Hazardous Index.

chemical species in the atmosphere after the intense firecrackers burning event. This was reported due to delayed effect of firecrackers emission and long residence time of atmospheric aerosols. In another study the mean aerosol residence times in the troposphere was calculated to be 1–25 days indicating the significance of delayed effect (Długosz-Lisiecka and Bem, 2012).

When we are dealing with PMs and their opposite effect on human health, the major factor that controls the path of particles into respiratory system is the aerodynamic diameter that depends upon the sources and formation mechanism of aerosols (Li et al., 2014; Castro et al., 2015; Chen et al., 2017). Cilia and mucus of respiratory tract filter particles with larger than 10 μm size but particles with less than 10 μm diameter are inhalable particles. They accommodate in the upper respiratory system but if inhaled it would be discarded by coughing and sneezing (Kim et al., 2015). Particles with size < 2.5 μm and < 1 μm are given more attention because of their extreme bad health impact due to their deeper approach into the human respiratory system (Dockery, 2001). Several studies conducted worldwide have reported occurrence of major diseases due to bad air quality, i.e., cardiovascular dysfunction, acute asthma, decreased lung function, lower resistance to foreign substances, etc. (Tapanainen et al., 2012). Some indoor and outdoor burning sources of aerosols have been reported carcinogenic (Vu et al., 2012; Canha et al., 2016). Air pollutants analysis at global level shows that atmospheric particulates are responsible for the 5%

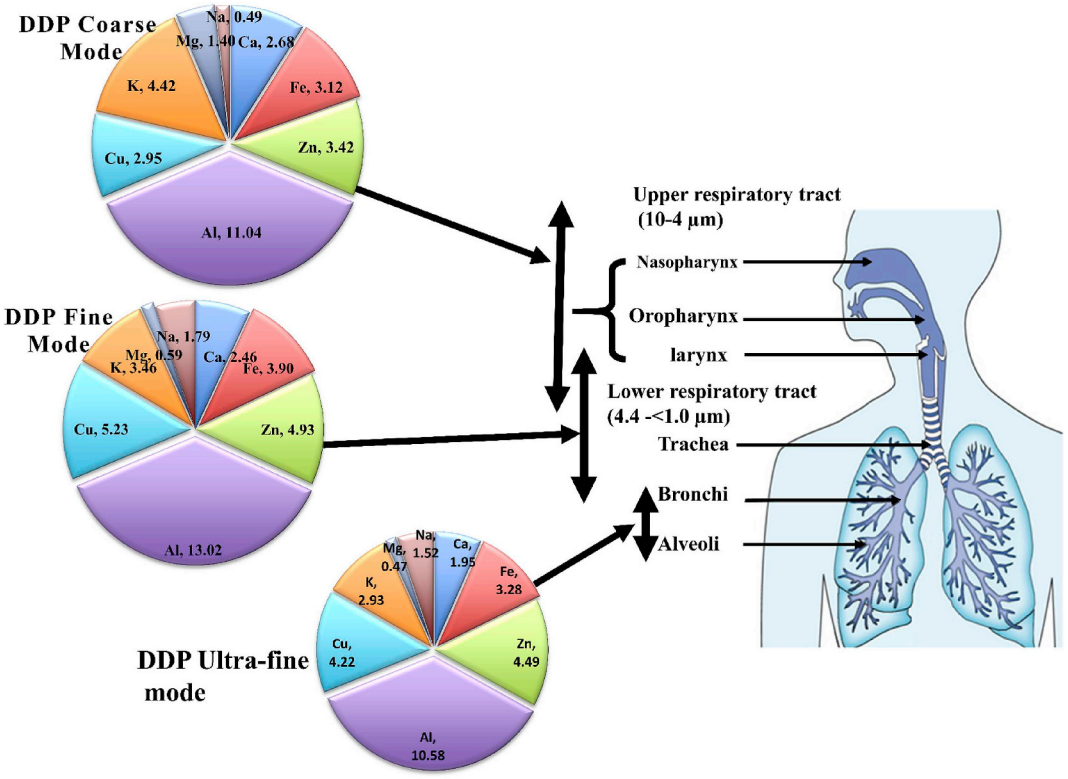

Fig. 9. Potential penetrations and health effect of metals (concentration in µg m^{-3}) and of aerosol emitted during fire cracker event at Raipur.

cancer cases (lung, trachea, bronchi), 2% cases of mortality due to cardio-respiratory problems and 1% mortality due to the respiratory infections (Bryce et al., 2005).

Once metals enter in the blood circulation via respiratory system, they can cause adverse health impact like Al may cause Parkinson's and Alzheimer's diseases, Osteomalacia, slow bone growth in infants, microcytic anemia etc. (Palazzolo et al., 2016; Williams et al., 2017). Aluminum is reported as a potential carcinogen, they are capable of causing fatal conditions like sinonasal and lung cancer. Once, Al enters in a blood circulation it can aggregate and affects the brain, kidneys, and liver. Cu is an essential element at low abundances. However, Cu inhalation may cause eosinophilia, alveolar migration of macrophages and formation of histiocytic and-caseating granulomas (Pappas, 2011). Copper may also cause eye irritation, nausea, chronic overexposure: damage to the liver and kidneys, anemia, acute copper poisoning: methemoglobinemia, liver injury, hemolytic anemia, epigastric pain, headache, dizziness, massive gastrointestinal bleeding, tachycardia, respiratory difficulty, liver and kidney failure, and death (Williams et al., 2017; Sawlani et al., 2019). The atmospheric loading of metals and their potential penetration over DDP, indicated unhealthier air quality and negative human health effects at eastern central India.

3.7. Comparison with other studies

Table 5 shows the abundances of coarse and fine particles during extreme firework display from reported literatures. The table shows that the abundance of fine particles was dominated over coarse particles for all the tracer metals except for K, which was dominated in coarse mode in the present work. Fireworks emitted new borne fine particles to the atmosphere that was the reason of high loading of fine particles. However, the gaseous precursors emitted from firecrackers burning also adhered onto the surface of the mineral dust particles justifying a valid reason for the significant contribution of the coarse mode loading of metals at Raipur during DDP. High abundance of metals was observed in the present work when compared with other studies of fireworks emissions events like Spring festival, Sant Joan firework, etc. events from different countries (Moreno et al., 2010; Deka and Hoque, 2014;Kong et al., 2015).

4. Conclusions

In the present work, size distributed aerosol samples were analyzed for metals and carbonaceous aerosols during BDP, DDP and ADP period in 2018 at eastern central India. In ultra-fine and fine mode particles size the abundance of metals during DDP was found to be high for Al followed by Cu, Zn, Fe, K, Ca, Na and Mg. Bimodal size distribution with intense fine mode peak was found for Na during DDP. A common bimodal size distribution with fine mode intense peak was found for K in all three events possibly due to biomass burning emissions, whereas high intense peak during DDP indicated couple of sources such as firecrackers emission along with biomass burning. During DDP, K and Ca were well correlated together, which was not found during BDP. It clearly indicated similar source of K and Ca, i.e., firecrackers burning, during DDP. Strong correlations between metal pairs Zn–Fe, Cu–Fe and Cu–Ca have been found. The salts of these metals are commonly mixed together in firecrackers to produce different colors on burning. This possibly gives a justifiable reason for such strong positive correlation among tracer metals in aerosols during Deepawali festival. The significant metals and carbonaceous aerosols were found during ADP in coarse fine and ultrafine size fractions. This should be significant residence time of atmospheric aerosols. Fire-crackers derived atmospheric aerosols were found to be existed several days after the firecrackers burning event and can alter the atmospheric chemistry. Fine particles can approach lower respiratory tract, i.e., trachea, and alveoli, so they are more harmful entities over coarse particles. The extreme fireworks in Deepawali festivals have apparently altered the compositions of size-distributed aerosols with elevated metals and organic matters loading. The contributions of SOC formed by gas to particle conversion gradually rose in firework days during aging processes. The particles emitted from fireworks obviously underwent aging processes as we have found

significant coarse mode loading of metals and carbonaceous aerosols during firework days. Aging of particles were characterized by heterogeneous reactions of directly emitted NO_x and SO_2 from fireworks on particles in the troposphere. The outcomes of this work will be useful to understanding the compositions of size distributed particles and aging processes of firework emissions. It also highlights the importance of controlling intensive firecrackers burning in order to protect air quality from deterioration and reduce the respiratory problems.

Disclaimer

The authors declare that they have no conflicts of interest.

Credit author statement

Mithlesh Mahilang: Data curation, Writing- Original draft preparation. Manas Kanti Deb: Conceptualization, Methodology, Software, Supervision. Jayant Nirmalakr: Visualization, Investigation. Shamsh Pervez: Writing- Software, Validation, Reviewing and Editing.

Acknowledgments

Authors are thankful to University Grant Commission's Special Assistance Programme, New Delhi, India [Letter No. F-540/7/DRS-II/2016 (SAP-I)], and Department of Science & Technology's Fund for Improvement of S&T Infrastructure, New Delhi, India [Letter No. SR/FST/CSI-259/2014(c)] New Delhi for financial support. The authors are thankful to the Chhattisgarh Council of Science & Technology Raipur, India [Endt. No. 2741/CCOST/MRP/2016] for financial support. Mithlesh Mahilang is also thankful to Pt. Ravishankar Shukla University, Raipur, C.G., India for providing university scholarship under the grant-in-aid, VR. No 1413/Fin/2016.

References

Aksu, A., 2015. Sources of metal pollution in the urban atmosphere (A case study: tuzla, Istabul). J. Environ. Health Sci. Engineer. 13, 79–85.

Allan, J.D., Williams, P.I., Morgan, W.T., Martin, C.L., Flynn, M.J., Lee, J., Nemitz, E., Phillips, G.J., Gallagher, M.W., Coe, H., 2010. Contributions from transport, solid fuel burning and cooking to primary organic aerosols in two UK cities. Atmos. Chem. Phys. 10, 647–668.

Ambade, B., 2018. The air pollution during Diwali festival by the burning of fireworks in Jamshedpur city, India. Urban Climate 26, 149–160.

Baptista, M.S., Vasconcelos, M.T., Cabral, J.P., Freitas, M.C., Pacheco, A.M., 2008. Copper, nickel, lead in lichens and tree bark transplants over different period of time. Environ. Pollut. 151, 408–413.

Barnett, A.G., Williams, G.M., Schwartz, J., Neller, A.H., Best, T.L., Petroeschevsky, A.L., Simpson, R.W., 2005. Air pollution and child respiratory health: a case-crossover study in Australia and New Zealand. Am. J. Respir. Crit. Care Med. 171, 1272–1278.

Bencardino, M., Andreoli, V., Castagna, J., D'Amore, F., Mannarino, V., Moretti, S., Naccarato, A., Pirrone, N., Sprovieri, F., 2018. Airborne particles during a firework festival in belvedere M.mo, south-western Italian coast. Open J. Air Pollut. 7, 156–180.

Bisht, D.S., Dumka, U.C., Kaskaoutis, D.G., Pipal, A.S., Srivastava, A.K., Soni, V.K., Attri, S.D., Sateesh, M., Tiwari, S., 2015. Carbonaceous aerosols and pollutants over Delhi urban environment: temporal evolution, source apportionment and radiative forcing. Sci. Total Environ. 521–522, 431–445. https://doi.org/10.1016/j.scitotenv.2015.03.083.

Bryce, J., Boschi-Pinto, C., Shibuya, K., Black, R.E., 2005. WHO child health epidemiology reference group, WHO estimates of the causes of death in children. Lancet 365, 1147–1152.

Camilleri, R., Vella, A.J., 2010. Effect of fireworks on ambient air quality in Malta. Atmos. Environ. 44, 4521–4527.

Canha, N., Lopes, I., Vicente, E.D., Vicente, A.M., Bandowe, B.A., Almeida, S.M., Alves, C.A., 2016. Mutagenicity assessment of aerosols in emissions from domestic combustion processes. Environ. Sci. Pollut. Res. 23, 10799–10807.

Castro, A., Calvo, A.I., Alves, C., Alonso-Blanco, E., Coz, E., Marques, L., Nunes, T., Fernandez-Guisuraga, J.M., Fraile, R., 2015. Indoor aerosol size distributions in a gymnasium. Sci. Total Environ. 524, 178–186.

Chen, L., Shi, M., Li, S., Gao, S., Zhang, H., Sun, Y., Mao, J., Bai, Z., Wang, Z., Zhou, J., 2017. Quantifying public health benefits of environmental strategy of $PM_{2.5}$ air quality management in Beijing–Tianjin–Hebei region, China. J. Environ. Sci. 57, 33–40.

Conticini, E., Frediani, B., Caro, D., 2020. Can atmospheric pollution be considered a co-factor in extremely high level of SARS-CoV-2 lethality in Northern Italy? Environ. Pollut. https://doi.org/10.1016/j.envpol.2020.114465.

Deka, P., Hoque, R.R., 2014. Diwali fireworks: early signs of impact on PM_{10} properties of rural Brahmaputra Valley. Aerosol Air Qual. Res. 14, 1752–1762.

Deshmukh, D.K., Deb, M.K., Verma, D., Nirmalkar, J., 2013. Seasonal air quality profile of size-segregated aerosols in the ambient air of a central Indian region. Bull. Environ. Contam. Toxicol. 91 (6), 704–710.

Deshmukh, D.K., Kawamura, K., Deb, M.K., Boreddy, S.K., 2017. Sources and formation processes of water-soluble dicarboxylic acids, ω-oxocarboxylic acids, α-dicarbonyls, and major ions in summer aerosols from eastern central India. J. Geophys. Res. Atmos. 122, 3630–3652.

Deshmukh, D.K., Kawamura, K., Lazaar, M., Kunwar, B., Boreddy, S.K., 2016. Dicarboxylic acids, oxoacids, benzoic acid, α-dicarbonyls, WSOC, OC, and ions in spring aerosols from Okinawa Island in the western North Pacific Rim: size distributions and formation processes. Atmos. Chem. Phys. 16, 5263–5282.

Długosz-Lisiecka, M., Bem, H., 2012. Determination of the mean aerosol residence times in the atmosphere and additional 210 Po input on the base of simultaneous determination of 7 Be, 22 Na, 210 Pb, 210 Bi and 210 Po in urban air. J. Radioanal. Nucl. Chem. 293 (1), 135–140.

Do, T.M., Wang, C.F., Hsieh, Y.K., Hsieh, H.F., 2012. Metals present in ambient air before and after a rework festival in yanshui, tainan, taiwan. Aerosol Air Qual. Res. 12, 981–993.

Dockery, D.W., 2001. Epidemiologic evidence of cardiovascular effects of particulate air pollution. Environ. Health Perspect. 109, 483–486.

Duan, N., 1982. Models for human exposure to air pollution. Environ. Int. 8 (1–6), 305–309.

Engling, G., Lee, J.J., Tsai, Y.W., Lung, S.C., Chou, C.C., Chan, C.Y., 2009. Size resolved anhydrosugar composition in smoke aerosol from controlled field burning of rice straw. Aerosol. Sci. Technol. 43, 662–672.

Fu, P.Q., Kawamura, K., Pavuluri, C.M., Swaminathan, T., Chen, J., 2010. Molecular characterization of urban organic aerosol in tropical India: contributions of primary emissions and secondary photooxidation. Atmos. Chem. Phys. 10, 2663–2689.

Godri, K.J., Green, D.C., Fuller, G.W., Dall'Osto, M., Beddows, D.C., Kelly, F.J., Harrison, R.M., Mudway, I.S., 2010. Particulate oxidative burden associated with fireworks activity. Environ. Sci. Technol. 44, 8295–8301.

Hamad, S., Green, D., Heo, J., 2016. Evaluation of health risk associated with fireworks activity at Central London. Air Qual. Atmos. Hlth. 9, 735–741.

Han, L., Zhuang, G., Cheng, S., Wang, Y., Li, J., 2007. Characteristics of re-suspended road dust and its impact on the atmospheric environment in Beijing. Atmos. Environ. 41, 7485–7499.

Haywood, J., Bush, M., Abel, S., Claxton, B., Coe, H., Crosier, J., Harrison, M., Macpherson, B., Naylor, M., Osborne, S., 2008. Prediction of visibility and aerosol within the operational met office united model. II: validation of model performance using observational data. Q. J. Roy. Meteorol. Soc. 134, 1817–1832.

Hillamo, R., Pacyna, J.M., Bartonova, A., 1988. Characterization of aerosols during long-range transport episodes of air pollution to Norway. J. Aerosol Sci. 19, 1257–1261.

Hirai, K., Yamazaki, Y., Okada, K., Furuta, S., Kubo, K., 2000. Acute eosinophilic pneumonia associated with smoke from fireworks. Intern. Med. 39, 401–403.

Huang, X.F., Chen, D.L., Lan, Z.J., Feng, N., He, L.Y., Yu, G.H., Luan, S.J., 2012. Characterization of organic aerosol in fine particles in a mega-city of South China: molecular composition, seasonal variation, and size distribution. Atmos. Res. 114, 28–37.

Jing, H., Li, Y.F., Zhao, J., Li, B., Sun, J., Chen, R., Gao, Y., Chen, C., 2014. Wide-range particle characterization and elemental concentration in Beijing aerosol during the 2013 Spring Festival. Environ. Pollut. 192, 204–211.

Joly, A., Smargiassi, A., Kosatsky, T., Fournier, M., Dabek-Zlotorzynska, E., Celo, V., Mathieu, D., Servranckx, R., D'amours, R., Malo, A., Brook, J., 2010. Characterization of particulate exposure during fireworks displays. Atmos. Environ. 44, 4325–4329.

Jurado, E., Dachs, J., Duarte, C.M., Simo, R., 2008. Atmospheric deposition of organic and black carbon to the global oceans. Atmos. Environ. 42 (34), 7931–7939.

Kanakidou, M., Seinfeld, J.H., Pandis, S.N., Barnes, I., Dentener, F.J., Facchini, M.C., Dingenen, R.V., Ervens, B., Nenes, A.N., Nielsen, C.J., Swietlicki, E., 2005. Organic aerosol and global climate modelling: a review. Atmos. Chem. Phys. 5, 1053–1123.

Kim, K.H., Kabir, E., Kabir, S., 2015. A review on the human health impact of airborne particulate matter. Environ. Int. 74, 136–143.

Koelmans, A.A., Jonker, M.T.O, Cornelissen, G., Bucheli, T.D., van Noort, P.C.M., Gustafsson, O., 2006. Black carbon: the reverse of its dark side. Chemosphere 63, 365–377. https://doi.org/10.1016/j.chemosphere.2005.08.034.

Kong, S.F., Li, L., Li, X.X., Yin, Y., Chen, K., Liu, D.T., Yuan, L., Zhang, Y.J., Shan, Y.P., Ji, Y.Q., 2015. The impacts of firework/burning at the Chinese Spring Festival on air quality: insights of tracers, source evolution and aging processes. Atmos. Chem. Phys. 15 (4), 2167–2184.

Levin, E.J., McMeeking, G.R., Carrico, C.M., Mack, L.E., Kreidenweis, S.M., Wold, C.E., Moosmüller, H., Arnott, W.P., Hao, W.M., Collett Jr., J.L., Malm, W.C., 2010. Biomass burning smoke aerosol properties measured during Fire Laboratory at Missoula Experiments (FLAME). J. Geophys. Res. Atmos. 115, D18210.

Li, B., Lei, X.N., Xiu, G.L., Gao, C.Y., Gao, S., Qian, N.S., 2015. Personal exposure to black carbon during commuting in peak and off-peak hours in Shanghai. Sci. Total Environ. 524–525, 237–245.

Li, L., Li, H., Zhang, X., Wang, L., Xu, L., Wang, X., Yu, Y., Zhang, Y., Cao, G., 2017. Online single particle measurement of fireworks pollution during Chinese New Year in Nanning. J. Environ. Sci. 53, 184–195.

Li, L., Li, H., Zhang, X., Wang, L., Xu, L., Wang, X., Yu, Y., Zhang, Y., Cao, G., 2014. Pollution characteristics and health risk assessment of benzene homologues in ambient air in the northeastern urban area of Beijing, China. J. Environ. Sci. 26, 214–223.

Li, N., Han, W., Wei, X., Shen, M., Sun, S., 2019. Chemical characteristics and human

health assessment of PM1 during the Chinese spring festival in changchun, northeast China. Atmos. Pollut. Res. 10 (6), 1823–1831.
Liu, B., He, M.M., Wu, C., Li, J., Li, Y., Lau, N.T., Yu, J.Z., Lau, A.K., Fung, J.C., Hoi, K.I., Mok, K.M., 2019. Potential exposure to fine particulate matter ($PM_{2.5}$) and black carbon on jogging trails in Macau. Atmos. Environ. 198, 23–33.
Liu, J., Chen, Y., Chao, S., Cao, H., Zhang, A., 2019. Levels and health risks of $PM_{2.5}$-bound toxic metals from firework/firecracker burning during festival periods in response to management strategies. Ecotoxicol. Environ. Saf. 171, 406–413.
Lu, F., Xu, D., Cheng, Y., Dong, S., Guo, C., Jiang, X., Zheng, X., 2015. Systematic review and meta-analysis of the adverse health effects of ambient $PM_{2.5}$ and PM_{10} pollution in the Chinese population. Environ. Res. 136, 196–204.
Mahilang, M., Deb, M.K., 2020. Seasonal variation and health implications of long-range transported and provincial size distributed aerosols at eastern central India. J. Indian Chem. Soc. 97, 85–100.
Matawle, J., Pervez, S., Dewangan, S., Tiwari, S., Bisht, D.S., Pervez, Y.F., 2014. $PM_{2.5}$ chemical source profiles of emissions resulting from industrial and domestic burning activities in India. Aerosol Air Qual. Res. 14, 2051–2066.
Matawle, J.L., Pervez, S., Deb, M.K., Shrivastava, A., Tiwari, S., 2018. $PM_{2.5}$ pollution from household solid fuel burning practices in Central India: 2. Application of receptor models for source apportionment. Environ. Geochem. Health 40, 145–161.
Miyazaki, Y., Kawamura, K., Jung, J., Furutani, H., Uematsu, M., 2011. Latitudinal distributions of organic nitrogen and organic carbon in marine aerosols over the western North Pacific. Atmos. Chem. Phys. 11 (7), 3037–3049.
Moreno, T., Querol, X., Alastuey, A., Amato, F., Pey, J., Pandolfi, M., Kuenzli, N., Bouso, L., Rivera, M., Gibbons, W., 2010. Effect of fireworks events on urban background trace metal aerosol concentrations: is the cocktail worth the show? J. Hazard Mater. 183, 945–949.
Moreno, T., Querol, X., Alastuey, A., Minguillón, M.C., Pey, J., Rodriguez, S., Miró, J.V., Felis, C., Gibbons, W., 2007. Recreational atmospheric pollution episodes: inhalable metalliferous particles from firework displays. Atmos. Environ. 41, 913–922.
Nirmalkar, J., Batmunkh, T., Jung, J., 2020. An optimized tracer-based approach for estimating organic carbon emissions from biomass burning in Ulaanbaatar, Mongolia. Atmos. Chem. Phys. 20, 3231–3247.
Nirmalkar, J., Deb, M.K., Deshmukh, D.K., Verma, S.K., 2013. Mass loading of size-segregated atmospheric aerosols in the ambient air during fireworks episodes in Eastern Central India. Bull. Environ. Contam. Toxicol. 90, 434–439.
Nirmalkar, J., Deshmukh, D.K., Deb, M.K., Chandrawanshi, S., Tiwari, S., 2016. Seasonal size distribution and possible health implications of atmospheric aerosols collected from a rural site of eastern central India. Atmos. Pollut. Res. 7 (2), 278–287.
Nirmalkar, J., Deshmukh, D.K., Deb, M.K., Tsai, Y.I., Pervez, S., 2019. Characteristics of aerosol during major biomass burning events over eastern central India in winter: a tracer-based approach. Atmos. Pollut. Res. 10 (3), 817–826.
Nriagu, J.O., Pacyna, J.M., 1998. Quantitative assessment of worldwide contamination of air, water, and soil by trace metals. Nature 333, 134–139.
Ott, W.R., 1982. Concepts of human exposure to air pollution. Environ. Int. 7, 179–196.
Palazzolo, D.L., Crow, A.P., Nelson, J.M., Johnson, R.A., 2017. Trace metals derived from electronic cigarette (ECIG) generated aerosol: potential problem of ECIG devices that contain nickel. Front. Physiol. 7, 1–17.
Pandey, P., Khan, A.H., Verma, A.K., Singh, K.A., Mathur, N., Kisku, G.C., Barman, S.C., 2012. Seasonal trends of $PM_{2.5}$ and PM_{10} in ambient air and their correlation in ambient air of Lucknow city, India. Bull. Environ. Contam. Toxicol. 88, 265–270.
Pani, S.K., Chantara, S., Khamkaew, C., Lee, C.T., Lin, N.H., 2019. Biomass burning in the northern peninsular Southeast Asia: aerosol chemical profile and potential exposure. Atmos. Res. 224, 180–195.
Pappas, R.S., 2011. Toxic elements in tobacco and in cigarette smoke: inflammation and sensitization. Metall 3, 1181–1198.
Pavuluri, C.M., Kawamura, K., Swaminathan, T., 2010. Water-soluble organic carbon, dicarboxylic acids, ketoacids, and α-dicarbonyls in the tropical Indian aerosols. J. Geophys. Res. Atmos. 115 (D11).
Perrino, C., Tiwari, S., Catrambone, M., Dalla Torre, S., Rantica, E., Canepari, S., 2011. Chemical characterization of atmospheric PM in Delhi, India, during different periods of the year including Diwali festival. Atmos. Pollut. Res. 2, 418–427.
Pervez, S., Chakrabarty, R.K., Dewangan, S., Watson, J.G., Chow, J.C., Matawle, J.L., 2014. Chemical speciation of aerosols and air quality degradation during the festival of lights (Diwali). Environ. Sci. Pollut. Res. 7, 92–99.
Pongpiachan, S., Hattayanone, M., Suttinun, O., Khumsup, C., Kittikoon, I., Hirunyatrakul, P., Cao, J., 2017. Assessing human exposure to PM10-bound polycyclic aromatic hydrocarbons during fireworks displays. Atmos. Pollut. Res. 8 (5), 816–827.
Pongpiachan, S., Paowa, T., 2015. Hospital out-and-in-patients as functions of trace gaseous species and other meteorological parameters in Chiang-Mai, Thailand. Aerosol Air Qual. Res. 15, 479–493.
Remskar, M., Tavcar, G., Skapin, S.D., 2015. Sparklers as a nanohazard: size distribution measurements of the nanoparticles released from sparklers. Air Qual. Atmos. Hlth. 8, 205–211.
Retama, A., Neria-Hernández, A., Jaimes-Palomera, M., Rivera-Hernandez, O., Sanchez-Rodriguez, M., Lopez-Medina, A., Velasco, E., 2019. Fireworks: a major source of inorganic and organic aerosols during Christmas and New Year in Mexico city. Atmos. Environ. X 2, 100013.
Sahu, R.K., Pervez, S., Chow, J.C., Watson, J.G., Tiwari, S., Panicker, A.S., Chakrabarty, R.K., Pervez, Y.F., 2018. Temporal and spatial variations of $PM_{2.5}$ organic and elemental carbon in Central India. Environ. Geochem. Health 40 (5), 2205–2222.
Samiksha, S., Raman, R.S., Nirmalkar, J., Kumar, S., Sirvaiya, R., 2017. PM_{10} and $PM_{2.5}$ chemical source profiles with optical attenuation and health risk indicators of paved and unpaved road dust in Bhopal, India. Environ. Pollut. 222, 477–485.
Sarkar, S., Khillare, P.S., Jyethi, D.S., Hasan, A., Parween, M., 2010. Chemical speciation of respirable suspended particulate matter during a major firework festival in India. J. Hazard Mater. 184, 321–330.
Sawlani, R., Agnihotri, R., Sharma, C., Patra, P.K., Dimri, A.P., Ram, K., Verma, R.L., 2019. The severe Delhi SMOG of 2016: a case of delayed crop residue burning, coincident firecracker emissions, and atypical meteorology. Atmos. Pollut. Res. 10 (3), 868–879.
Segura, S., Estellés, V., Esteve, A.R., Utrillas, M.P., Martínez-Lozano, J.A., 2013. Analysis of a severe pollution episode in Valencia (Spain) and its effect on ground level particulate matter. J. Aerosol Sci. 56, 41–52.
Singh, M., Jaques, P.A., Sioutas, C., 2002. Size Distribution and diurnal characteristics of particle-bound metals in source and receptor sites of the Los Angeles Basin. Atmos. Environ. 36, 1675–1689.
Sotiropoulou, R.E.P., Tagaris, E., Pilinis, C., Anttila, T., Kulmala, M., 2006. Modeling new particle formation during air pollution episodes: impacts on aerosol and cloud condensation nuclei. Aerosol Sci. Technol. 40, 557–572.
Tandon, A., Yadav, S., Attri, A.K., 2008. City-wide sweeping a source for respirable particulate matter in the atmosphere. Atmos. Environ. 42, 1064–1069.
Tang, X., Zhang, X., Wang, Z., Ci, Z., 2016. Water-soluble organic carbon (WSOC) and its temperature-resolved carbon fractions in atmospheric aerosols in Beijing. Atmos. Res. 181, 200–210.
Tao, J., Cheng, T., Zhang, R., Cao, J., Zhu, L., Wang, Q., Luo, L., Zhang, L., 2013. Chemical composition of $PM_{2.5}$ at an urban site of Chengdu in southwestern China. Adv. Atmos. Sci. 30, 1070–1084. https://doi.org/10.1007/s00376-012-2168-7.
Tapanainen, M., Jalava, P.I., Mäki-Paakkanen, J., Hakulinen, P., Lamberg, H., Ruusunen, J., Tissari, J., Jokiniemi, J., Hirvonen, M.R., 2012. Efficiency of log wood combustion affects the toxicological and chemical properties of emission particles. Inhal. Toxicol. 24, 343–355.
Terry, J.P., Jia, G., Boldi, R., Khan, S., 2018. The Delhi 'gas chamber': smog, air pollution and the health emergency of November 2017. Weather 73, 348–352.
Tsai, H.H., Chien, L.H., Yuan, C.S., Lin, Y.C., Jen, Y.H., Ie, I.R., 2012. Influences of fireworks on chemical characteristics of atmospheric fine and coarse particles during Taiwan's. Lantern Festival. Atmos. Environ. 62, 256–264.
Turpin, B.J., Huntzicker, J.J., 1991. Secondary formation of organic aerosol in the Los Angeles Basin: a descriptive analysis of organic and elemental carbon concentrations. Atmos. Environ. 25, 207–215.
UNICEF, 2016. Clean the air for children. In: The Impact of Air Pollution on Children. UNICEF. https://www.unicef.org/publications/index_92957.html.
US EPA, 2011. Exposure Factors Handbook.
US EPA (United State Environmental Protection Agency), 2001. Risk Assessment Guidance for Superfund: Volume III — Part A, Process for Conducting Probabilistic Risk Assessment. EPA 540-R-02-002. US Environmental Protection Agency, Washington, D.C.
Vecchi, R., Bernardoni, V., Cricchio, D., D'Alessandro, A., Fermo, P., Lucarelli, F., Nava, S., Piazzalunga, A., Valli, G., 2008. The impact of fireworks on airborne particles. Atmos. Environ. 42, 1121–1132.
Verma, S.K., Deb, M.K., Suzuki, Y., Tsai, Y.I., 2010. Ion chemistry and source identification of coarse and fine aerosols in an urban area of eastern central India. Atmos. Res. 95, 65–76.
Vu, B., Alves, C.A., Gonçalves, C., Pio, C., Gonçalves, F., Pereira, R., 2012. Mutagenicity assessment of aerosols in emissions from wood combustion in Portugal. Environ. Pollut. 166, 172–181.
Wang, S., Pavuluri, C.M., Ren, L., Fu, P., Zhang, Y.L., Liu, C.Q., 2018. Implications for biomass/coal combustion emissions and secondary formation of carbonaceous aerosols in North China. RSC Adv. 8, 38108–38117.
Wang, X., Wang, W., Yang, L., Gao, X., Nie, W., Yu, Y., Xu, P., Zhou, Y., Wang, Z., 2012. The secondary formation of inorganic aerosols in the droplet mode through heterogenous aqueous reaction under haze conditions. Atmos. Environ. 63, 68–76.
Wang, Y., Zhuang, G., Xu, C., An, Z., 2007. The air pollution caused by the burning of fireworks during the lantern festival in Beijing. Atmos. Environ. 41, 417–431.
Williams, M., Bozhilov, K., Ghai, S., Talbot, P., 2017. Elements including metals in the atomizer and aerosol of disposable electronic cigarettes and electronic hookahs. PloS One 12 (4), e0175430. https://doi.org/10.1371/journal.pone.0175430.
Yamasoe, M.A., Artaxo, P., Miguel, A.H., Allen, A.G., 2000. Chemical composition of aerosol particles from direct emissions of vegetation fires in the Amazon Basin: water-soluble species and trace elements. Atmos. Environ. 34, 1641–1653.
Yang, L., Gao, X., Wang, X., Nie, W., Wang, J., Gao, R., Xu, P., Shou, Y., Zhang, Q., Wang, W., 2014. Impacts of firecracker burning on aerosol chemical characteristics and human health risk levels during the Chinese New Year Celebration in Jinan, China. Sci. Total Environ. 476–477, 57–64.
Zhang, J., Wang, S., Guo, Y., Xu, D., Gong, Y., Tang, X., 2013. Supercritical water oxidation of polyvinyl alcohol and desizing wastewater: influence of NaOH on the organic decomposition. J. Environ. Sci. 25 (8), 1583–1591.
Zhu, D., Wan, L., 2019. Characteristics and formation mechanism of a serious haze event in autumn 2017 in Harbin, China. Air Qual. Atmos. Hlth. 12 (10), 1169–1179.